

COVER PAGE

Document downloaded by @DAEL

Sun Nov 8 02:50:07 2026
For personal use

When automatic English translation is provided, only the original document is authentic.
The EAA cannot be held responsible of any translation error

Bibliographical reference

Viscothermal Longitudinal Wave Propagation in Non-Uniform Shear Liquid Flow Confined by Constant Temperature Pipeline and Implications for Ultrasonic Flow Meter, Yong Chen, Yiyong Huang and Xiaoqian Chen, Acta Acustica **vol. 99** (Number 6), 2013, pp. 875-889

DOI
https://doi.org/10.3813/AAA.918667

Acta Acustica united with Acustica
Vol. 99 (2013) 875 – 889

DOI 10.3813/AAA.918667

Viscothermal Longitudinal Wave Propagation in Non-Uniform Shear Liquid Flow Confined by Constant Temperature Pipeline and Implications for Ultrasonic Flow Meter

Yong Chen, Yiyong Huang, Xiaoqian Chen
Institute of Space Technology, College of Aerospace Science and Engineering,
National University of Defense Technology, 410073, Changsha, China.
literature.chen@gmail.com, yiyong_h@sina.com, chenxiaoqian@nudt.edu.cn

Summary
Viscothermal longitudinal wave propagation in incompressible viscous liquid with non-uniform shear flow confined by rigid pipeline wall of constant temperature is mathematically formulated, which is a set of coupled fourth-order nonlinear differential equations. Based on Bessel-Fourier theory, a general solution in the form of Bessel-Fourier sequences, which are orthogonal and complete in Lebesgue Space, is proposed to transform the fourth-order nonlinear differential equations to a set of homogeneous linear algebraic equations. Then acoustic wave number can be solved using the existence condition of non-trivial solution to the homogeneous linear algebraic equations, leading to the vanishment of the corresponding determinant which can be numerically calculated by various iteration methods. Based on the proposed scheme, phase velocity and attenuation of viscothermal longitudinal wave is numerically analysed in shear flow. In the end, measurement performance of ultrasonic flow meter based on wave propagation is investigated.

PACS no. 43.20.Bi, 43.20.Mv, 43.28.Py, 43.35.Ud, 47.35.Rs, 43.35.Yb

1. Introduction

Ultrasonic longitudinal wave propagation in thermal-viscous fluid is receiving considerable attention in recent years. One early model of sound propagation in circular tubes is the classical Kirchhoff equation [1] from 1868 that includes the effect of viscosity as well as heat conduction. Kirchhoff himself derived the complete solution of the problem from the basic equations in the form of a very complicated transcendental equation in the case of stationary fluid flow. More than 50 years later an approximate solution to a simplified version of Kirchhoff's equation was found by Zwikker and Kosten [2] for circular geometry. Research efforts by several consecutive authors can be found in [3, 4, 5, 6, 7, 8, 9].

However, none of the early work treated the effect of non-uniform shear flow. On the assumption that the radial wave velocity has negligible influence upon the axial wave propagation, Peat [10] firstly gave an approximate solution using a variational principle, and later analyzed the wave motion in the presence of temperature graident [11]. Based on the simplified model proposed by Peat, Jeong and IH [12] presented a numerical solution in the form of Runge-Kutta and shooting method. Astley and Cummings [13] showed a discretization numerical calculation strategy based on the finite element method with nine-noded isoparametric mesh. For analytical solution, while IH, Park and Kim [14] provided an analytical solution in terms of Confluent Hypergeometric function, Dokumaci [15, 16] introduced a quasi-analytical solution for uniform shear flow in circular pipeline, and then a solution in the form of double Fourier Sine series [17] for non-uniform shear flow in rectangular waveguide. Willatzen [18] considered the phase shift and attenuation of acoustic wave in moving fluid using Frobenius power series expansion method. Based on the work of Peat, Cummings and Dokumaci [19], Knutsson and Abom [20, 21] considered the effect of turbulent damping [22] using Weighted Residuals method proposed by Eversman [23, 24, 25, 26].

The common assumption of the above mentioned contributions is that acoustic radial velocity is much smaller than the axial component, and radial changes are much larger than axial variations. As a result, the radial component of the particle velocity is neglected [21]. However, it has been investigated that inclusion of the radial component of the acoustic velocity within the analysis has an observable effect upon the wave propagation [12, 27]. Through power series expansion, Peat and Kirby [27] gave an approximate solution for wave propagation including the effect of radial velocity, but the gradient of acoustic

Received 8 June 2012,
accepted 1 August 2013.

© S. Hirzel Verlag · EAA

Document downloaded by @DAEL, 2026-11-08 02:50:09 - personal use only

pressure in the radial direction is assumed be zero and the dissipation function is simplified [28, 29, 30]. By expressing the velocity field as a combination of scalar and rotational potentials, Elvira-Segura [31] and later Baik, Jiang and Leighton [32] showed a general analytical solution for circular waveguide and Sorokin [33, 34] for rectangular waveguide. Unfortunately, these solutions are only for stationary flow and the state of fluid is assumed to be isentropic. In the previous work [35], present authors investigated isentropic longitudinal wave propagation in uniform shear flow.

On the other hand, little is known on the wave propagation in the thermal-viscous liquid fluid with complex flow profile. In the framework of inviscid fluid, Willatzen [36, 37] gave an analysis of wave propagation including temperature gradient, and then investigated the influence of temperature gradient on ultrasonic flow measurement [38, 39, 40, 41, 42] in laminar flow. However, in Willatzen's work [36, 37], the dynamics of temperature is not considered, the governing equation of wave propagation is only valid for low Mach inviscid fluid flow, and then wave propagation in turbulent flow is not addressed.

Based on the previous research [35, 43], viscothermal longitudinal wave propagation [8, 44, 45, 46, 47, 48, 49, 50, 51, 52, 53, 54, 55] in rigid cylindrical pipeline in the presence of non-uniform shear flow is deduced using the potential theory [8, 44, 45, 46, 47, 48, 49], leading to a set of coupled fourth-order nonlinear differential equations. Using Bessel-Fourier Theory [56, 57, 58, 59, 60, 61, 62, 63, 64, 65, 66, 67, 68, 69, 70, 71, 72], a general solution in the form of Bessel-Fourier sequence, which is orthogonal and complete in Lebesgue Space, is proposed to transform the coupled fourth-order nonlinear differential equations to homogeneous linear algebraic equations. As a result, the problem is converted to the problem of nontrivial solution existence of homogeneous linear equations, resulting in the vanishment of corresponding determinant [73, 74, 75, 76]. Based on the established method, longitudinal wave propagation in laminar and turbulent flow is analyzed. Finally, parametric analysis of ultrasonic flow meter performance [35, 36, 37] is investigated in laminar and turbulent flow. The layout of the paper is as follows. In section 2, viscothermal longitudinal wave propagation in non-uniform shear liquid flow confined by rigid cylindrical pipeline is mathematically deduced from the incompressible N-S equation, the continuity equation, the equation of state, and the energy equation, and then a general solution based on the Bessel-Fourier theory is presented. Section 3 gives a comprehensive parametric analysis of viscothermal longitudinal wave propagation in shear flow. Meanwhile, measurement performance of ultrasonic flow meter based on wave propagation is discussed. The last section concludes the paper.

2. Theory of viscothermal longitudinal wave propagation

In this section, viscothermal longitudinal wave propagation in incompressible homogeneous viscous liquid fluid confined by rigid cylindrical pipeline is mathematically formulated as shown in Figure 1, then a novel solution based on Bessel-Fourier theory is proposed.

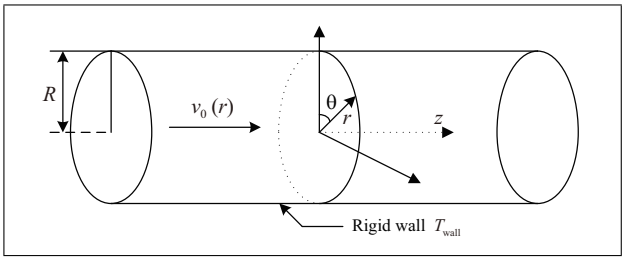


Figure 1. Waveguide with cylindrical coordinate system. R is the radius of the rigid pipeline with constant temperature T_{wall}, and $v_0(r)$ is the shear flow profile.

2.1. Mathematical formulation

The governing equation of viscothermal longitudinal wave propagation in incompressible thermal-viscous fluid are [28, 29]
conservation of mass,

$$\frac{\partial \rho}{\partial t} + \nabla \cdot \left(\rho v\right) = 0, \tag{1}$$

conservation of momentum,

$$\frac{\partial v}{\partial t} + \left(\boldsymbol{v} \cdot \nabla\right)\boldsymbol{v} = -\frac{\nabla p}{\rho} + \frac{\eta}{\rho}\nabla^2 \boldsymbol{v}, \tag{2}$$

conservation of energy without external heat source,

$$\rho T\left(\frac{\partial s}{\partial t} + \left(\boldsymbol{v} \cdot \nabla\right)s\right) = \kappa_{th}\nabla^2 T + \frac{\eta}{2}\sum_{ij=1}^{3}\left(\frac{\partial v_i}{\partial x_j} + \frac{\partial v_j}{\partial x_i}\right)^2, \tag{3}$$

where ρ, p, T, s, and $\boldsymbol{v} = [v_1, v_2, v_3]$ denote fluid density, pressure, temperature, entropy, and velocity, η and κ_{th} are the shear viscosity and thermal conductivity which are assumed to be constant in this paper. From the work of Blokhintzev [77], s can be expressed as a function of p and ρ,

$$\frac{\partial s}{\partial t} = \frac{c_p}{T}\frac{\partial T}{\partial t} - \frac{\beta}{\rho}\frac{\partial p}{\partial t}, \quad \nabla s = \frac{c_p}{T}\nabla T - \frac{\beta}{\rho}\nabla p, \tag{4}$$

where β is the coefficient of volume thermal expansion and c_p is the constant-pressure heat capacity per unit mass. Substituting equation (4) into (3) gives [30]

$$\frac{\partial T}{\partial t} + \left(\boldsymbol{v} \cdot \nabla\right)T = \frac{\kappa_{th}}{\rho c_p}\nabla^2 T + \frac{\beta T}{\rho c_p}\left(\frac{\partial p}{\partial t} + \left(\boldsymbol{v} \cdot \nabla\right)p\right) + \frac{\eta}{2\rho c_p}\sum_{ij=1}^{3}\left(\frac{\partial v_i}{\partial x_j} + \frac{\partial v_j}{\partial x_i}\right)^2, \tag{5}$$

as shown by White [30], the condition $\beta T = 1$ holds in perfect gas which is assumed in the analysis of viscothermal wave propagation in the literature [10, 78]. However, β is usually smaller than $1/T$ and may even be negative in liquid, for imperfect gas, β can be considerably larger

Document downloaded by @DAEL, 2026-11-08 02:50:09 - personal use only

than $1/T$ at high pressure. To get a general mathematical formulation, the general equation of thermodynamics is adopted in this paper.

When the incompressible fluid experiences a small-amplitude disturbance, its ambient physical variables (denoted by a subscript zero) are modified to

$$\begin{aligned} \boldsymbol{v} &= \boldsymbol{v}_0 + \boldsymbol{v}', \quad p = p_0 + p', \quad \rho = \rho_0 + \rho', \\ T &= T_0 + T', \quad \rho_0 = \text{const.} \end{aligned} \tag{6}$$

Substituting equation (6) into equations (1), (2), and (5) gives the dynamics of viscothermal wave propagation in incompressible fluid

$$\begin{aligned} &\frac{\partial \rho'}{\partial t} + \big(\boldsymbol{v}_0 \cdot \nabla\big)\rho' + \rho_0 \nabla \cdot \boldsymbol{v}' = 0, \\ &\frac{\partial \boldsymbol{v}'}{\partial t} + \big(\boldsymbol{v}' \cdot \nabla\big)\boldsymbol{v}_0 + \big(\boldsymbol{v}_0 \cdot \nabla\big)\boldsymbol{v}' = \\ &\quad - \frac{\nabla p'}{\rho_0} + \frac{\eta}{\rho_0}\nabla^2 \boldsymbol{v}' - \frac{\rho'}{\rho_0^2}\big(-\nabla p_0 + \eta \nabla^2 \boldsymbol{v}_0\big), \\ &\frac{\partial T'}{\partial t} + \big(\boldsymbol{v}' \cdot \nabla\big)T_0 + \big(\boldsymbol{v}_0 \cdot \nabla\big)T' = \\ &\quad - \frac{\kappa_{th}}{\rho_0 c_p}\nabla^2 T' + \frac{\beta T_0}{\rho c_p}\Big(\frac{\partial p'}{\partial t} + \big(\boldsymbol{v}_0 \cdot \nabla\big)p'\Big) \\ &\quad + \frac{\beta(\boldsymbol{v}_0 \cdot \nabla)p_0}{\rho_0 c_p}T' \\ &\quad + \frac{\eta}{\rho_0 c_p}\sum_{ij=1}^{3}\Big(\frac{\partial v_{0i}}{\partial x_i} + \frac{\partial v_{0j}}{\partial x_i}\Big)\Big(\frac{\partial v_i'}{\partial x_i} + \frac{\partial v_j'}{\partial x_i}\Big) \\ &\quad - \frac{\rho'}{\rho_0^2 c_p}\Bigg(\kappa_{th}\nabla^2 T_0 + \beta T_0\big(\boldsymbol{v}_0 \cdot \nabla\big)p_0 \\ &\qquad + \frac{\eta}{2}\sum_{ij=1}^{3}\Big(\frac{\partial v_{0i}}{\partial x_i} + \frac{\partial v_{0j}}{\partial x_i}\Big)^2\Bigg), \end{aligned} \tag{7}$$

and the steady flow is governed by

$$\begin{aligned} \nabla \cdot \big(\rho_0 \boldsymbol{v}_0\big) &= 0, \\ \big(\boldsymbol{v}_0 \cdot \nabla\big)\boldsymbol{v}_0 &= -\frac{\nabla p_0}{\rho_0} + \frac{\eta}{\rho_0}\nabla^2 \boldsymbol{v}_0, \\ \big(\boldsymbol{v}_0 \cdot \nabla\big)T_0 &= -\frac{\kappa_{th}}{\rho_0 c_p}\nabla^2 T_0 + \frac{\beta T_0}{\rho c_p}\big(\boldsymbol{v}_0 \cdot \nabla\big)p_0 \\ &\quad + \frac{\eta}{2\rho_0 c_p}\sum_{ij=1}^{3}\Big(\frac{\partial v_{0i}}{\partial x_i} + \frac{\partial v_{0j}}{\partial x_i}\Big)^2. \end{aligned} \tag{8}$$

Assume the flow is taken to be axially symmetric, several special flow cases [79], such as axial shear flow, solid body swirl, and free vortex swirl, exist for steady flow. In the literature, the axial shear flow, i.e., $\boldsymbol{v}_0 = [0, 0, v_0(r)]$ as shown in Figure 1, has been examined by many authors and is used for validation of the present paper. Substitution into equation (8) gives

$$\begin{aligned} \big(\boldsymbol{v}_0 \cdot \nabla\big)\boldsymbol{v}_0 &= -\frac{\nabla p_0}{\rho_0} + \frac{\eta}{\rho_0}\nabla^2 \boldsymbol{v}_0 = 0, \\ \big(\boldsymbol{v}_0 \cdot \nabla\big)T_0 &= \frac{\kappa_{th}}{\rho_0 c_p}\nabla^2 T_0 + \frac{\beta T_0}{\rho c_p}\big(\boldsymbol{v}_0 \cdot \nabla\big)p_0 \\ &\quad + \frac{\eta}{\rho_0 c_p}\Big(\frac{\mathrm{d}v_0(r)}{\mathrm{d}r}\Big)^2, \quad T_0\big|_{r=R} = T_{\text{wall}}, \end{aligned} \tag{9}$$

where T_{wall} is the temperature near the wall as shown in Figure 1. From the first equation of equation (9), it can be inferred

$$\nabla p_0 = \eta \nabla^2 \boldsymbol{v}_0. \tag{10}$$

Insertion of equation (10) into the second equation of equation (9) gives

$$\begin{aligned} \big(\boldsymbol{v}_0 \cdot \nabla\big)T_0 &= \frac{\kappa_{th}}{\rho_0 c_p}\nabla^2 T_0 + \frac{\beta T_0}{\rho c_p}\frac{\eta v_0(r)}{r}\frac{\mathrm{d}}{\mathrm{d}r}\Big(r\frac{\mathrm{d}v_0(r)}{\mathrm{d}r}\Big) \\ &\quad + \frac{\eta}{\rho_0 c_p}\Big(\frac{\mathrm{d}v_0(r)}{\mathrm{d}r}\Big)^2, \quad T_0\big|_{r=R} = T_{\text{wall}}. \end{aligned} \tag{11}$$

Substitution of equations (8) and (9) into equation (7) yields

$$\begin{aligned} &\frac{\partial \rho'}{\partial t} + \big(\boldsymbol{v}_0 \cdot \nabla\big)\rho' + \rho_0 \nabla \cdot \boldsymbol{v}' = 0, \\ &\frac{\partial \boldsymbol{v}'}{\partial t} + \big(\boldsymbol{v}' \cdot \nabla\big)\boldsymbol{v}_0 + \big(\boldsymbol{v}_0 \cdot \nabla\big)\boldsymbol{v}' = -\frac{\nabla p'}{\rho_0} + \frac{\eta}{\rho_0}\nabla^2 \boldsymbol{v}', \\ &\frac{\partial T'}{\partial t} + \big(\boldsymbol{v}' \cdot \nabla\big)T_0 + \big(\boldsymbol{v}_0 \cdot \nabla\big)T' = \\ &\quad - \frac{\kappa_{th}}{\rho_0 c_p}\nabla^2 T' + \frac{\beta T_0}{\rho c_p}\Big(\frac{\partial p'}{\partial t} + \big(\boldsymbol{v}' \cdot \nabla\big)p_0 + \big(\boldsymbol{v}_0 \cdot \nabla\big)p'\Big) \\ &\quad + \frac{\beta(\boldsymbol{v}_0 \cdot \nabla)p_0}{\rho_0 c_p}T' \\ &\quad + \frac{\eta}{\rho_0 c_p}\sum_{ij=1}^{3}\Big(\frac{\partial v_{0i}}{\partial x_i} + \frac{\partial v_{0j}}{\partial x_i}\Big)\Big(\frac{\partial v_i'}{\partial x_i} + \frac{\partial v_j'}{\partial x_i}\Big) \\ &\quad - \frac{\rho'}{\rho_0}\big(\boldsymbol{v}_0 \cdot \nabla\big)T_0. \end{aligned} \tag{12}$$

Treating ρ_0 as a function of p' and T' obtains [29, 77]

$$\rho' = \frac{1}{c_0^2(T_0)}p' - \beta \rho_0 T', \tag{13}$$

where $c_0(T_0)$ is the isothermal velocity of sound and a function of steady temperature T_0. Insertion of equation (13) into equation (12) gives

$$\begin{aligned} &\frac{\partial p'}{\partial t} + \big(\boldsymbol{v}_0 \cdot \nabla\big)p' - \beta \rho_0 c_0^2(T_0)\Big(\frac{\partial T'}{\partial t} + \big(\boldsymbol{v}_0 \cdot \nabla\big)T'\Big) \\ &\qquad + \rho_0 c_0^2(T_0)\nabla \cdot \boldsymbol{v}' = 0, \\ &\frac{\partial \boldsymbol{v}'}{\partial t} + \big(\boldsymbol{v}' \cdot \nabla\big)\boldsymbol{v}_0 + \big(\boldsymbol{v}_0 \cdot \nabla\big)\boldsymbol{v}' = -\frac{\nabla p'}{\rho_0} + \frac{\eta}{\rho_0}\nabla^2 \boldsymbol{v}', \\ &\frac{\partial T'}{\partial t} + \big(\boldsymbol{v}' \cdot \nabla\big)T_0 + \big(\boldsymbol{v}_0 \cdot \nabla\big)T' = \\ &\quad - \frac{\kappa_{th}}{\rho_0 c_p}\nabla^2 T' + \frac{\beta T_0}{\rho c_p}\Big(\frac{\partial p'}{\partial t} + \big(\boldsymbol{v}' \cdot \nabla\big)p_0 + \big(\boldsymbol{v}_0 \cdot \nabla\big)p'\Big) \\ &\quad + \frac{\beta(\boldsymbol{v}_0 \cdot \nabla)p_0}{\rho_0 c_p}T' \\ &\quad + \frac{\eta}{\rho_0 c_p}\sum_{ij=1}^{3}\Big(\frac{\partial v_{0i}}{\partial x_i} + \frac{\partial v_{0j}}{\partial x_i}\Big)\Big(\frac{\partial v_i'}{\partial x_i} + \frac{\partial v_j'}{\partial x_i}\Big) \\ &\quad - \frac{p' - \beta \rho_0 c_0^2(T_0)T'}{\rho_0 c_0^2(T_0)}\big(\boldsymbol{v}_0 \cdot \nabla\big)T_0. \end{aligned} \tag{14}$$

Document downloaded by @DAEL, 2026-11-08 02:50:09 - personal use only

The divergence of the second equation shows

$$\begin{aligned}
&\frac{\partial p'}{\partial t} + \big(\boldsymbol{v}_0 \cdot \nabla\big)p' - \beta\rho_0 c_0^2(T_0)\Big(\frac{\partial T'}{\partial t} + \big(\boldsymbol{v}_0 \cdot \nabla\big)T'\Big) \\
&\qquad + \rho_0 c_0^2(T_0)\nabla \cdot \boldsymbol{v}' = 0, \\
&\frac{\partial \nabla \cdot \boldsymbol{v}'}{\partial t} + \nabla\big((\boldsymbol{v}' \cdot \nabla)\boldsymbol{v}_0 + (\boldsymbol{v}_0 \cdot \nabla)\boldsymbol{v}'\big) = \\
&\quad - \frac{\nabla^2 p'}{\rho_0} + \frac{\eta}{\rho_0}\nabla^2(\nabla \cdot \boldsymbol{v}'), \\
&\frac{\partial T'}{\partial t} + \big(\boldsymbol{v}' \cdot \nabla\big)T_0 + \big(\boldsymbol{v}_0 \cdot \nabla\big)T' = \\
&\quad - \frac{\kappa_{th}}{\rho_0 c_p}\nabla^2 T' + \frac{\beta T_0}{\rho c_p}\Big(\frac{\partial p'}{\partial t} + \big(\boldsymbol{v}' \cdot \nabla\big)p_0 + \big(\boldsymbol{v}_0 \cdot \nabla\big)p'\Big) \\
&\quad + \frac{\beta(\boldsymbol{v}_0 \cdot \nabla)p_0}{\rho_0 c_p}T' \\
&\quad + \frac{\eta}{\rho_0 c_p}\sum_{ij=1}^{3}\Big(\frac{\partial v_{0i}}{\partial x_i} + \frac{\partial v_{0j}}{\partial x_i}\Big)\Big(\frac{\partial v'_i}{\partial x_i} + \frac{\partial v'_j}{\partial x_i}\Big) \\
&\quad - \frac{p' - \beta\rho_0 c_0^2(T_0)T'}{\rho_0 c_0^2(T_0)}\big(\boldsymbol{v}_0 \cdot \nabla\big)T_0.
\end{aligned} \tag{15}$$

For longitudinal wave propagation [8, 44, 45, 46, 47, 48, 49, 50, 51, 52, 53, 54, 55], the fluid velocity can be expressed as the gradient of a scalar potential Φ,

$$\boldsymbol{v}' = \nabla\Phi. \tag{16}$$

Substituting equation (16) into equation (15) yields

$$\begin{aligned}
&\frac{\partial p'}{\partial t} + \big(\boldsymbol{v}_0 \cdot \nabla\big)p' - \beta\rho_0 c_0^2(T_0)\Big(\frac{\partial T'}{\partial t} + \big(\boldsymbol{v}_0 \cdot \nabla\big)T'\Big) \\
&\qquad + \rho_0 c_0^2(T_0)\nabla\Phi = 0, \\
&\frac{\partial \nabla^2\Phi}{\partial t} + \nabla\big((\boldsymbol{v}' \cdot \nabla)\boldsymbol{v}_0 + (\boldsymbol{v}_0 \cdot \nabla)\boldsymbol{v}'\big) = \\
&\quad - \frac{\nabla^2 p'}{\rho_0} + \frac{\eta}{\rho_0}\nabla^2\nabla^2\Phi, \\
&\frac{\partial T'}{\partial t} + \big(\boldsymbol{v}' \cdot \nabla\big)T_0 + \big(\boldsymbol{v}_0 \cdot \nabla\big)T' = \\
&\quad - \frac{\kappa_{th}}{\rho_0 c_p}\nabla^2 T' + \frac{\beta T_0}{\rho c_p}\Big(\frac{\partial p'}{\partial t} + \big(\boldsymbol{v}' \cdot \nabla\big)p_0 + \big(\boldsymbol{v}_0 \cdot \nabla\big)p'\Big) \\
&\quad + \frac{\beta(\boldsymbol{v}_0 \cdot \nabla)p_0}{\rho_0 c_p}T' \\
&\quad + \frac{\eta}{\rho_0 c_p}\sum_{ij=1}^{3}\Big(\frac{\partial v_{0i}}{\partial x_i} + \frac{\partial v_{0j}}{\partial x_i}\Big)\Big(\frac{\partial v'_i}{\partial x_i} + \frac{\partial v'_j}{\partial x_i}\Big) \\
&\quad - \frac{p' - \beta\rho_0 c_0^2(T_0)T'}{\rho_0 c_0^2(T_0)}\big(\boldsymbol{v}_0 \cdot \nabla\big)T_0.
\end{aligned} \tag{17}$$

For monochromatic acoustic ($\exp(\mathrm{i}\omega t)$) propagation, with ω ($= 2\pi f$) being the angular frequency, equation (17) is modified to

$$\begin{aligned}
&\mathrm{j}\omega p' + \big(\boldsymbol{v}_0 \cdot \nabla\big)p' - \beta\rho_0 c_0^2(T_0)\Big(\frac{\partial T'}{\partial t} + \big(\boldsymbol{v}_0 \cdot \nabla\big)T'\Big) \\
&\qquad + \rho_0 c_0^2(T_0)\nabla\Phi = 0, \\
&\mathrm{j}\omega\nabla\Phi + \nabla\big((\boldsymbol{v}' \cdot \nabla)\boldsymbol{v}_0 + (\boldsymbol{v}_0 \cdot \nabla)\boldsymbol{v}'\big) = \\
&\quad - \frac{\nabla^2 p'}{\rho_0} + \frac{\eta}{\rho_0}\nabla^2\nabla^2\Phi, \\
&\frac{\partial T'}{\partial t} + \big(\boldsymbol{v}' \cdot \nabla\big)T_0 + \big(\boldsymbol{v}_0 \cdot \nabla\big)T' = \\
&\quad \frac{\kappa_{th}}{\rho_0 c_p}\nabla^2 T' + \frac{\beta T_0}{\rho c_p}\Big(\frac{\partial p'}{\partial t} + \big(\boldsymbol{v}' \cdot \nabla\big)p_0 + \big(\boldsymbol{v}_0 \cdot \nabla\big)p'\Big) \\
&\quad + \frac{\beta(\boldsymbol{v}_0 \cdot \nabla)p_0}{\rho_0 c_p}T' \\
&\quad + \frac{\eta}{\rho_0 c_p}\sum_{ij=1}^{3}\Big(\frac{\partial v_{0i}}{\partial x_i} + \frac{\partial v_{0j}}{\partial x_i}\Big)\Big(\frac{\partial v'_i}{\partial x_i} + \frac{\partial v'_j}{\partial x_i}\Big) \\
&\quad - \frac{p' - \beta\rho_0 c_0^2(T_0)T'}{\rho_0 c_0^2(T_0)}\big(\boldsymbol{v}_0 \cdot \nabla\big)T_0
\end{aligned} \tag{18}$$

for axial symmetric wave characterized by the presence of velocity components in the radial and axial directions, in circular cylindrical coordinate in Figure 1, the acoustic pressure, scalar potential, and temperature have the following formulation

$$\begin{aligned}
p'(r, z, t) &= \varphi_p(r)\exp\big(\mathrm{j}(\omega t - k_z z)\big), \\
\Phi(r, z, t) &= \varphi_\Phi(r)\exp\big(\mathrm{j}(\omega t - k_z z)\big), \\
T'(r, z, t) &= \varphi_T(r)\exp\big(\mathrm{j}(\omega t - k_z z)\big),
\end{aligned} \tag{19}$$

where k_z is the axial wave number, and its real and imaginary components denote individually the information of phase velocity and attention. Moreover, $\varphi_p(r)$, $\varphi_\Phi(r)$, and $\varphi_T(r)$ are piecewise smooth functions satisfying

$$\begin{aligned}
&\int_0^R \sqrt{r}\varphi_p(r) < +\infty, \ \big|\varphi_p(r)\big| < +\infty, \\
&\int_0^R \sqrt{r}\varphi_\Phi(r) < +\infty, \ \big|\varphi_\Phi(r)\big| < +\infty, \\
&\int_0^R \sqrt{r}\varphi_T(r) < +\infty, \ \big|\varphi_T(r)\big| < +\infty.
\end{aligned} \tag{20}$$

Substituting equation (19) into equation (16) gives the velocity components [57, 80]

$$\boldsymbol{v}' = \begin{bmatrix} v'_r \\ v'_z \end{bmatrix} = \begin{bmatrix} \dfrac{\mathrm{d}\varphi_\Phi(r)}{\mathrm{d}r} \\ -\mathrm{j}k_z\varphi_\Phi(r) \end{bmatrix}\exp\big(\mathrm{j}(\omega t - k_z z)\big), \tag{21}$$

and expanding equation (18) in circular cylindrical coordinate for axial symmetric condition, using equation (10), (19), and (21), gives

$$\begin{aligned}
&\mathrm{j}\big(\omega - k_z v_0(r)\big)\big(\varphi_p(r) - \beta\rho_0 c_0^2(T_0)\varphi_T(r)\big) \\
&\quad + \rho_0 c_0^2(T_0)\Big(\frac{1}{r}\frac{\mathrm{d}}{\mathrm{d}r}\Big(r\frac{\mathrm{d}\varphi_\Phi(r)}{\mathrm{d}r}\Big) - k_z^2\varphi_\Phi(r)\Big) = 0,
\end{aligned}$$

Document downloaded by @DAEL, 2026-11-08 02:50:09 - personal use only

$$
\begin{aligned}
&\mathrm{j}\big(\omega - k_z v_0(r)\big)\Big(\frac{1}{r}\frac{\mathrm{d}}{\mathrm{d}r}\Big(r\frac{\mathrm{d}\varphi_\Phi(r)}{\mathrm{d}r}\Big) - k_z^2\varphi_\Phi(r)\Big) - \mathrm{j}2k_z\frac{\mathrm{d}v_0(r)}{\mathrm{d}r}\frac{\mathrm{d}\varphi_\Phi(r)}{\mathrm{d}r}\\
&\quad = -\frac{1}{\rho_0}\Big(\frac{1}{r}\frac{\mathrm{d}}{\mathrm{d}r}\Big(r\frac{\mathrm{d}\varphi_p(r)}{\mathrm{d}r}\Big) - k_z^2\varphi_p(r)\Big)\\
&\quad + \frac{\eta}{\rho_0}\Big(\frac{1}{r}\frac{\mathrm{d}}{\mathrm{d}r}\Big(r\frac{\mathrm{d}}{\mathrm{d}r}\Big(\frac{1}{r}\frac{\mathrm{d}}{\mathrm{d}r}\Big(r\frac{\mathrm{d}\varphi_\Phi}{\mathrm{d}r}\Big) - k_z^2\varphi_\Phi(r)\Big)\Big)\\
&\quad - k_z^2\Big(\frac{1}{r}\frac{\mathrm{d}}{\mathrm{d}r}\Big(r\frac{\mathrm{d}\varphi_\Phi}{\mathrm{d}r}\Big) - k_z^2\varphi_\Phi(r)\Big)\Big),\\
&\mathrm{j}\big(\omega - k_z v_0(r)\big)\varphi_T(r) + \frac{\partial T_0}{\partial r}\frac{\mathrm{d}\varphi_\Phi(r)}{\mathrm{d}r} - \mathrm{j}k_z\frac{\partial T_0}{\partial r}\varphi_\Phi(r)\\
&\quad = \frac{\kappa_{th}}{\rho_0 c_p}\Big(\frac{1}{r}\frac{\mathrm{d}}{\mathrm{d}r}\Big(r\frac{\mathrm{d}\varphi_T(r)}{\mathrm{d}r}\Big) - k_z^2\varphi_T(r)\Big)\\
&\quad - \frac{\varphi_p(r) - \beta\rho_0 c_0^2(T_0)\varphi_\prime(r)}{\rho_0 c_0^2(T_0)}\frac{\partial T_0}{\partial r}v_0(r)\\
&\quad + \frac{\beta T_0}{\rho_0 c_p}\Big(\mathrm{j}\big(\omega - k_z v_0(r)\big)\varphi_p(r)\\
&\quad - \mathrm{j}k_z\frac{\eta}{r}\frac{\mathrm{d}}{\mathrm{d}r}\Big(r\frac{\mathrm{d}v_0(r)}{\mathrm{d}r}\Big)\varphi_\Phi(r)\Big)\\
&\quad + \frac{\beta}{\rho_0 c_p}\frac{\eta v_0(r)}{r}\frac{\mathrm{d}}{\mathrm{d}r}\Big(r\frac{\mathrm{d}v_0(r)}{\mathrm{d}r}\Big)\varphi_T(r)\\
&\quad - \frac{\mathrm{j}4\eta k_z}{\rho_0 c_p}\frac{\mathrm{d}v_0(r)}{\mathrm{d}r}\frac{\mathrm{d}\varphi_\Phi}{\mathrm{d}r},
\end{aligned}
\tag{22}
$$

and T_0 are calculated by equation (11).

From analysis of Astley and Cummings [13], the walls can be treated to be rigid and have much greater thermal conductivity than the fluid. Therefore, the boundary conditions are

$$
\frac{\partial p'}{\partial r} = 0 \ \text{ at } \ r = R, \quad v_r' = T' = 0 \ \text{ at } \ r = R. \tag{23}
$$

Substituting equations (19) and (21) into equation (23) gives the boundary condition

$$
\begin{aligned}
&\frac{\mathrm{d}\varphi_p(r)}{\mathrm{d}r}\Big|_{r=R} = 0, \qquad \frac{\mathrm{d}\varphi_\Phi(r)}{\mathrm{d}r}\Big|_{r=R} = 0,\\
&\frac{\mathrm{d}\varphi_T(r)}{\mathrm{d}r}\Big|_{r=R} = 0.
\end{aligned}
\tag{24}
$$

2.2. Solution based on Bessel-Fourier theory

In this section, a general method based on Bessel-Fourier theory is introduced to settle the coupled fourth-order nonlinear differential equations with boundary condition on the condition that functions, to be solved, are piecewise smooth.

Following Bessel-Fourier theory in [56, 57, 58, 59, 60, 61, 62, 63, 64, 65, 66, 67, 68, 69, 70, 71, 72], the smooth functions φ_p, φ_Φ and φ_T in equation (19) can be generally represented as

$$
\begin{aligned}
\varphi_p(r) &= \sum_{n=1}^{\infty} C_n^p J_{M1}(\lambda_n^p r) + D_n^p Y_{M1}(\lambda_n^p r),\\
\varphi_\Phi(r) &= \sum_{n=1}^{\infty} C_n^\Phi J_{M2}(\lambda_n^\Phi r) + D_n^\Phi Y_{M2}(\lambda_n^\Phi r),\\
\varphi_T(r) &= \sum_{n=1}^{\infty} C_n^T J_{M3}(\lambda_n^T r) + D_n^T Y_{M3}(\lambda_n^T r),
\end{aligned}
\tag{25}
$$

where the first-kind of Bessel function $J_{M1}(\lambda_n^p r)$ and second-kind of Bessel function $Y_{M1}(\lambda_n^p r)$ are selected to be orthogonal and complete in Lebesgue space while $M1$ denotes the order of Bessel function. Similar requirement are imposed on $J_{M2}(\lambda_n^\Phi r)$ and $Y_{M2}(\lambda_n^\Phi r)$, as well as $J_{M3}(\lambda_n^T r)$ and $Y_{M3}(\lambda_n^T r)$. From equation (20), it is shown that φ_p, φ_Φ and φ_T are bounded in the interval $r \in [0, R]$, then equation (25) can be simplified to

$$
\begin{aligned}
\varphi_p(r) &= \sum_{n=1}^{\infty} C_n^p J_{M1}(\lambda_n^p r),\\
\varphi_\Phi(r) &= \sum_{n=1}^{\infty} C_n^\Phi J_{M2}(\lambda_n^\Phi r),\\
\varphi_T(r) &= \sum_{n=1}^{\infty} C_n^T J_{M3}(\lambda_n^T r).
\end{aligned}
\tag{26}
$$

Substituting equation (26) into the boundary conditions in equation (24) obtains

$$
\begin{aligned}
&\frac{\mathrm{d}J_{M1}(\lambda_n^p r)}{\mathrm{d}r}\Big|_{r=R} = 0, \quad \frac{\mathrm{d}J_{M2}(\lambda_n^\Phi r)}{\mathrm{d}r}\Big|_{r=R} = 0,\\
&\frac{\mathrm{d}J_{M3}(\lambda_n^T r)}{\mathrm{d}r}\Big|_{r=R} = 0.
\end{aligned}
\tag{27}
$$

In this paper the zeroth-order Bessel function with $M1 = M2 = M3$ are selected, and then there is $\lambda_n^p = \lambda_n^\Phi$, thus equation (26) can be simplified to

$$
\begin{aligned}
\varphi_p(r) &= \sum_{n=1}^{\infty} C_n^p J_0(\lambda_n^p r),\\
\varphi_\Phi(r) &= \sum_{n=1}^{\infty} C_n^\Phi J_0(\lambda_n^p r),\\
\varphi_T(r) &= \sum_{n=1}^{\infty} C_n^T J_0(\lambda_n^T r),
\end{aligned}
\tag{28}
$$

and the orthogonal and complete Bessel-Fourier sequences can be obtained with

$$
J_1(\lambda_n^p R) = 0, \qquad J_0(\lambda_n^T R) = 0. \tag{29}
$$

From Appendix A1, the orthogonality has the following property

$$
\int_0^R J_0(\lambda_n^p r) J_0(\lambda_m^p r) r\,\mathrm{d}r = \begin{cases} 0, & m \neq n,\\ R^2 J_0^2(\lambda_m^p R)/2, & m = n, \end{cases} \tag{30}
$$

$$
\int_0^R J_0(\lambda_n^T r) J_0(\lambda_m^T r) r\,\mathrm{d}r = \begin{cases} 0, & m \neq n,\\ R^2 J_1^2(\lambda_m^T R)/2, & m = n. \end{cases} \tag{31}
$$

Moreover, the corresponding coefficients can be obtained by

$$
\begin{aligned}
C_n^p &= \frac{2}{J_0^2(\lambda_n^p R)}\int_0^R \varphi_p(r) J_0(\lambda_n^p r) r\,\mathrm{d}r,\\
C_n^\Phi &= \frac{2}{J_0^2(\lambda_n^p R)}\int_0^R \varphi_\Phi(r) J_0(\lambda_n^p r) r\,\mathrm{d}r,
\end{aligned}
\tag{32}
$$

Document downloaded by @DAEL, 2026-11-08 02:50:09 - personal use only

$$C_n^T = \frac{2}{J_0^2(\lambda_n^T R)} \int_0^R \varphi_T(r) J_0(\lambda_n^T r) r \, \mathrm{d}r,$$

showing that these coefficients are independent on the radius coordinate.

It should be noticed that φ_p, φ_Φ and φ_T are the unknown functions to be determined in this paper. From the formulation in Bessel-Fourier sequences, the problem of solving the unknown functions are then converted to the problem of solving the corresponding coefficients. Substituting equation (28) into equation (22) gives

$$\sum_{n=1}^{\infty} \mathrm{j}\big(\omega - k_z v_0(r)\big)\big[C_n^p J_0(\lambda_n^p r) - \beta\rho_0 c_0^2(T_0) C_n^T J_0(\lambda_n^T r)\big] - \rho_0 c_0^2(T_0)\big((\lambda_n^p)^2 + k_z^2\big) C_n^\Phi J_0(\lambda_n^p r) = 0,$$

$$\begin{aligned}\sum_{n=1}^{\infty} &-\mathrm{j}\big(\omega - k_z v_0(r)\big)\big((\lambda_n^p)^2 + k_z^2\big) C_n^\Phi J_0(\lambda_n^p r) \\ &+ \mathrm{j}2\lambda_n^p k_z \frac{\mathrm{d}v_0(r)}{\mathrm{d}r} C_n^\Phi J_1(\lambda_n^p r) \\ &= \sum_{n=1}^{\infty} \frac{\big((\lambda_n^p)^2 + k_z^2\big)}{\rho_0} C_n^p J_0(\lambda_n^p r) \\ &\quad + \frac{\eta}{\rho_0}\big((\lambda_n^p)^2 + k_z^2\big)^2 C_n^\Phi J_0(\lambda_n^p r),\end{aligned}$$

$$\begin{aligned}\sum_{n=1}^{\infty} &\mathrm{j}\big(\omega - k_z v_0(r)\big) C_n^T J_0(\lambda_n^T r) \\ &- \lambda_n^p \frac{\partial T_0}{\partial r} J_1(\lambda_n^p r) C_n^\Phi - \mathrm{j}k_z \frac{\partial T_0}{\partial r} J_1(\lambda_n^p r) C_n^\Phi \\ &= \sum_{n=1}^{\infty} \frac{-\kappa_{th} C_n^T}{\rho_0 c_p}\big((\lambda_n^T)^2 + k_z^2\big) J_0(\lambda_n^T r) \\ &\quad - \frac{C_n^p J_0(\lambda_n^p r) - \beta\rho_0 c_0^2(T_0) C_n^T J_0(\lambda_n^p r)}{\rho_0 c_0^2(T_0)} \frac{\partial T_0}{\partial z} v_0(r) \\ &\quad + \frac{\beta T_0}{\rho_0 c_p}\Big(\mathrm{j}\big(\omega - k_z v_0(r)\big) C_n^p \\ &\qquad - \mathrm{j}\eta k_z \frac{\mathrm{d}}{r\mathrm{d}r}\Big(r\frac{\mathrm{d}v_0(r)}{\mathrm{d}r}\Big) C_n^\Phi\Big) J_0(\lambda_n^p r) \\ &\quad + \frac{\beta}{\rho_0 c_p} \frac{\eta v_0(r)}{r} \frac{\mathrm{d}}{\mathrm{d}r}\Big(r\frac{\mathrm{d}v_0(r)}{\mathrm{d}r}\Big) C_n^T J_0(\lambda_n^T r) \\ &\quad + \frac{\mathrm{j}4\eta k_z \lambda_n^p}{\rho_0 c_p} \frac{\mathrm{d}v_0(r)}{\mathrm{d}r} J_1(\lambda : n^p r) C_n^\Phi.\end{aligned} \tag{33}$$

after some rearrangements, there is

$$\begin{aligned}\sum_{n=1}^{\infty} \mathrm{j}\omega C_n^p J_0(\lambda_n^p r) &= \sum_{n=1}^{\infty} \mathrm{j}k_z C_n^p v_0(r) J_0(\lambda_n^p r) \\ &\quad + \rho_0\big((\lambda_n^p)^2 + k_z^2\big) C_n^\Phi c_0^2(T_0) J_0(\lambda_n^p r) \\ &\quad - \mathrm{j}\beta\rho_0 k_z C_n^T v_0(r) c_0^2(T_0) J_0(\lambda_n^T r),\end{aligned}$$

$$\begin{aligned}&\sum_{n=1}^{\infty} \big((\lambda_n^p)^2 + k_z^2\big) \\ &\quad \cdot \Big(\frac{C_n^p}{\rho_0} + \Big(\mathrm{j}\omega + \frac{\eta}{\rho_0}\big((\lambda_n^p)^2 + k_z^2\big)\Big) C_n^\Phi\Big) J_0(\lambda_n^p r) \\ &= \sum_{n=1}^{\infty} \mathrm{j}\big((\lambda_n^p)^2 + k_z^2\big) C_n^\Phi v_0(r) J_0(\lambda_n^p r) \\ &\qquad + \mathrm{j}2\lambda_n^p k_z C_n^\Phi \frac{\mathrm{d}^{v_0(r)} r}{\mathrm{d}\boldsymbol{J}^{v_0(r)}}_1 (\lambda_n^p r),\end{aligned}$$

$$\begin{aligned}&\sum_{n=1}^{\infty} \mathrm{j}\omega C_n^T J_0(\lambda_n^T r) + \frac{-\kappa_{th} C_n^T}{\rho_0 c_p}\big((\lambda_n^T)^2 + k_z^2\big)^2 J_0(\lambda_n^T r) \\ &= \sum_{n=1}^{\infty} C_n^p\Big(\frac{\mathrm{j}\beta}{\rho_0 c_p}\big(\omega T_0 - k_z T_0 v_0(r)\big) \\ &\qquad - \frac{v_0(r)}{\rho_0 c_0^2(T_0)} \frac{\partial T_0}{\partial z}\Big) J_0(\lambda_n^p r) \\ &\qquad + \Big(\Big(\mathrm{j}k_z + \beta\frac{\partial T_0}{\partial z}\Big) v_0(r) \\ &\qquad\quad + \frac{\beta\eta}{\rho_0 c_p} \frac{v_0(r)}{r} \frac{\mathrm{d}}{\mathrm{d}r}\Big(r\frac{\mathrm{d}v_0(r)}{\mathrm{d}r}\Big)\Big) C_n^T J_0(\lambda_n^T r) \\ &\qquad + C_n^\Phi\Big(\lambda_n^p \frac{\partial T_0}{\partial r} J_1(\lambda_n^p r) + \mathrm{j}k_z \frac{\partial T_0}{\partial z} J_0(\lambda_n^p r) \\ &\qquad\quad + \frac{\mathrm{j}4\eta k_z \lambda_n^p}{\rho_0 c_p} \frac{\mathrm{d}v_0(r)}{\mathrm{d}r} J_1(\lambda_n^p r) \\ &\qquad\quad - \mathrm{j}k_z \frac{\beta\eta}{\rho_0 c_p} \frac{T_0}{r} \frac{\mathrm{d}}{r\mathrm{d}r}\Big(r\frac{\mathrm{d}v_0(r)}{\mathrm{d}r}\Big) C_n^\Phi\Big) J_0(\lambda_n^p r)\Big).\end{aligned} \tag{34}$$

Multiplying $J_0(\lambda_m^p r) r$ to first two equations and $J_0(\lambda_m^T r) r$ to the third equation of equation (33), then using orthogonal property of Bessel-Fourier theory (equations 30–31), and integrating in the interval give

$$\begin{aligned}&\mathrm{j}\omega C_m^p \sum_{n=1}^{\infty} \mathrm{j}k_z H_m^n C_n^p + \rho_0\big((\lambda_n^p)^2 + k_z^2\big) I_m^n C_n^\Phi \\ &\qquad + \mathrm{j}\beta\rho_0 k_z J_m^n C_n^T = 0, \\ &\frac{\big((\lambda_n^p)^2 + k_z^2\big)}{\rho_0} C_m^p + E_m^\Phi C_m^\Phi \\ &\qquad + \sum_{n=1}^{\infty} \mathrm{j}\big((\lambda_n^p)^2 k_z H_m^n + k_z^3 H_m^n + 2\lambda_n^p k_z K_m^n\big) C_n^\Phi = 0, \\ &E_m^T C_m^T + \sum_{n=1}^{\infty} \Big(\frac{\mathrm{j}\beta}{\rho_0 c_p}\big(\omega L_m^n + k_z M_m^n\big) + \frac{N_m^n}{\rho_0}\Big) C_n^p \\ &+ \Big(\mathrm{j}k_z O_m^n + \beta P_m^n + \frac{\beta\eta}{\rho_0 c_p} Q_m^n\Big) C_n^T \\ &+ \Big(\lambda_n^p S_m^n + \mathrm{j}k_z V_m^n + \frac{\mathrm{j}4\eta\lambda_n^p k_z}{\rho_0 c_p} W_m^n + \mathrm{j}k_z \frac{\beta\eta}{\rho_0 c_p} Y_m^n\Big) C_n^\Phi = 0,\end{aligned} \tag{35}$$

where

$$A_m^p = -\frac{2}{R^2 J_0^2(\lambda_m^p R)}, \qquad A_m^T = -\frac{2}{R^2 J_1^2(\lambda_m^T R)},$$

$$H_m^n = A_m^p \int_0^R v_0(r) J_0(\lambda_n^p r) J_0(\lambda_m^p r)\, r \mathrm{d}r,$$

Document downloaded by @DAEL, 2026-11-08 02:50:09 - personal use only

$$
\begin{aligned}
I_m^n &= A_m^p \int_0^R c_0^2(T_0) J_0(\lambda_n^p r) J_0(\lambda_m^p r)\, r\mathrm{d}r,\\
J_m^n &= A_m^p \int_0^R -v_0(r) c_0^2(T_0) J_0(\lambda_n^T r) J_0(\lambda_m^p r)\, r\mathrm{d}r,\\
K_m^n &= A_m^p \int_0^R \frac{\mathrm{d}v_0(r)}{\mathrm{d}r} J_1(\lambda_n^p r) J_0(\lambda_m^p r)\, r\mathrm{d}r,\\
L_m^n &= A_m^T \int_0^R T_0 J_0(\lambda_n^p r) J_0(\lambda_m^T r)\, r\mathrm{d}r,\\
M_m^n &= A_m^T \int_0^R -T_0 v_0(r) J_0(\lambda_n^p r) J_0(\lambda_m^p r)\, r\mathrm{d}r,\\
N_m^n &= A_m^T \int_0^R -\frac{\partial T_0}{\partial z} \frac{v_0(r)}{c_0^2(r)} J_0(\lambda_n^p r) J_0(\lambda_m^T r)\, r\mathrm{d}r,\\
O_m^n &= A_m^T \int_0^R v_0(r) J_0(\lambda_n^T r) J_0(\lambda_m^T r)\, r\mathrm{d}r,\\
P_m^n &= A_m^T \int_0^R \frac{\partial T_0}{\partial z} v_0(r) J_0(\lambda_n^T r) J_0(\lambda_m^T r)\, r\mathrm{d}r,\\
Q_m^n &= A_m^T \int_0^R \frac{v_0(r)}{r} \frac{\mathrm{d}}{\mathrm{d}r}\Big(r \frac{\mathrm{d}v_0(r)}{\mathrm{d}r}\Big) J_0(\lambda_n^T r) J_0(\lambda_T^p r)\, r\mathrm{d}r,\\
S_m^n &= A_m^T \int_0^R \frac{\partial T_0}{\partial r} J_1(\lambda_n^p r) J_0(\lambda_m^T r)\, r\mathrm{d}r,\\
V_m^n &= A_m^T \int_0^R \frac{\partial T_0}{\partial z} J_0(\lambda_n^p r) J_0(\lambda_m^T r)\, r\mathrm{d}r,\\
W_m^n &= A_m^T \int_0^R \frac{\mathrm{d}v_0(r)}{\mathrm{d}r} J_1(\lambda_n^p r) J_0(\lambda_m^T r)\, r\mathrm{d}r,\\
Y_m^n &= A_m^T \int_0^R -\frac{T_0}{r} \frac{\mathrm{d}}{\mathrm{d}r}\Big(r \frac{\mathrm{d}v_0(r)}{\mathrm{d}r}\Big) J_0(\lambda_n^T r) J_0(\lambda_T^p r)\, r\mathrm{d}r,\\
E_m^\Phi &= \big((\lambda_m^p)^2 + k_z^2\big)\Big(\mathrm{j}\omega + \frac{\eta}{\rho_0}\big((\lambda_m^p)^2 + k_z^2\big)\Big),\\
E_m^T &= \mathrm{j}\omega + \frac{\kappa_{th}}{\rho_0 c_p}\big((\lambda_m^T)^2 + k_z^2\big)\Big).
\end{aligned}
\tag{36}
$$

Using Bessel-Fourier sequence, the fourth-order nonlinear differential equations in equation (22) are transformed to homogeneous algebraic equations where the variables to be solved are the coefficients (C_m^p, C_m^Φ and C_m^T) of the Bessel sequences and the axial wave number k_z.

2.3. Calculation procedure

Obviously, given specific shear flow profile $v_0(r)$, acoustic frequency ω, waveguide pipeline R, fluid density ρ_0, and the orthogonal Bessel-Fourier sequences $J_0(\lambda_n^p r)$ and $J_0(\lambda_n^T r)$ ($n = 1, \ldots, N$) calculated by equation (29), expanding equation (35) gives a set of algebraic equations with the unknown parameters C_n^p, C_n^Φ and C_n^T and the axial wave number k_z. A careful investigation reveals that the number of unknown variables in equation (35) is $3N + 1$ while the number of homogeneous algebraic equations is $3N$, leading to the conclusion that the problem can't been solved until another condition is given. The reason is that the potential Φ, acoustic pressure p', and temperature T' are determined by the energy from the acoustic source which is given by the present boundary condition.

While the specific coefficients C_n^p, C_n^Φ and C_n^T and can't be solved from equation (35), the axial wave number k_z can be obtained. It is clearly that expanding equation (35) gives a set of homogeneous linear equations expressed by

$$
\boldsymbol{G}(k_z)\boldsymbol{X} = 0, \tag{37}
$$

where $\boldsymbol{X} = [C_1^p \ \ldots \ C_N^p \ C_1^\Phi \ \ldots \ C_N^\Phi \ C_1^T \ \ldots \ C_N^T]$ is the unknown variables, and $\boldsymbol{G}(k_z)$ is a matrix of a dimension $3N \times 3N$. From equation (32), it can be seen that the coefficients of Bessel-Fourier sequences don't vanish at the same time, and then $\boldsymbol{X} \neq 0$. As a result, the existence condition of non-trivial solution for homogeneous linear equations of equation (37) is that the corresponding determinant vanishes, leading to anonlinear function of theaxial wave number k_z expressed by

$$
\det\big(\boldsymbol{G}(k_z)\big) = 0, \tag{38}
$$

which can be solved by various numerical methods in the literature. See Appendix A2 for parabolic Newton numerical iteration method of equation (38) while the derivative of equation (38) can be obtained using the property of matrix determinant as shown by Meyer [75].

3. Numeric calculation and discussion

In this section, viscothermal longitudinal wave propagation in pipeline with constanttemperature is numerically-analysedand measurement performance [35, 36, 37] of ultrasonic flowmeter based on wave propagation is investigated.The pipeline with constant temperaturecanbe expressed by

$$
T_0 = \overline{T}_0 + g(r), \tag{39}
$$

where $\overline{T}_0$ is the temperature near the pipeline wall. In the case of water [81], the constant parameters used $\overline{T}_0 = 293\,\mathrm{K}$, $\rho_0 = 1000\,\mathrm{kg/m^3}$, $\eta = 1 \cdot 10^{-3}\,\mathrm{Kg/m/s}$, $c_p = 4181.8\,\mathrm{J/kg/K}$), $\kappa_{th} = 0.5984\,\mathrm{W/K/m}$, and $\beta = 0.206 \cdot 10^{-3}/\mathrm{K}$. As a result, assuming $\beta T_0 \approx \beta \overline{T}_0$ along the radius coordinate in the pipeline, substituting equation (39) into equation (11) gives

$$
\begin{aligned}
&\kappa_{th} \frac{1}{r} \frac{\mathrm{d}}{\mathrm{d}r}\Big(r \frac{\mathrm{d}g(r)}{\mathrm{d}r}\Big)\\
&\quad + \frac{\beta \overline{T}_0 \eta v_0(r)}{r} \frac{\mathrm{d}}{\mathrm{d}r}\Big(r \frac{\mathrm{d}v_0(r)}{\mathrm{d}r}\Big) + \eta\Big(\frac{\mathrm{d}v_0(r)}{\mathrm{d}r}\Big)^2 = 0,
\end{aligned}
\tag{40}
$$

and the sound isothermal velocity $c(T_0)$ [82] can be calculated by

$$
\begin{aligned}
c(T_0) \approx\ & 1449.2 + 4.6(T_0 - 273) - 0.055(T_0^2 73)^2\\
&+ 0.00029(T_0 - 273)^3,
\end{aligned}
\tag{41}
$$

and then $c(\overline{T}_0) = 1521.5\,\mathrm{m/s}$. For incompressible viscous fluid, the axial wave number k_z can be expressed as

$$
k_z = \alpha - \mathrm{j}\beta, \qquad \beta \gg 0, \tag{42}
$$

Document downloaded by @DAEL, 2026-11-08 02:50:09 - personal use only

where β is the attenuation factor and phase velocity c_p is

$$c_p = \omega/\alpha. \tag{43}$$

In the end, to quantitatively analyze the performance of ultrasonic flow meter based on wave propagation, the deviation of measurement E_n (measurement error) is introduced as shown in [35, 83, 84, 85, 86, 87],

$$E_n = \frac{\Delta t_n - \Delta t_0}{\Delta t_0}, \tag{44}$$

where Δt_0 is the transit time difference of the fundamental mode in inviscid fluid expressed by

$$\Delta t_0 = \frac{2LU}{c(\overline{T}_0)^2}, \tag{45}$$

where U is the average amplitude value of the velocity, and Δt_n is the propagation time difference of the nth order mode in upstream and downstream wave propagation,

$$\Delta t_n = \frac{L}{2\pi f}\left(\alpha_n^{\text{upstream}} - \alpha_m^{\text{downstream}}\right), \tag{46}$$

with L being the pipeline length. Substituting equations (45) and (46) into equation (44) gives

$$E_n = \frac{c(\overline{T}_0)^2\left(\alpha_n^{\text{upstream}} - \alpha_m^{\text{downstream}}\right)}{4\pi f U} - 1. \tag{47}$$

3.1. Phase velocity and attenuation

From the previous work [18, 83, 84, 85, 86], the shear flow profile can be expressed by

$$v_0(r) = \tau U + (1-\tau)2U\left(1 - \frac{r^2}{R^2}\right), \tag{48}$$

where

$$\tau = 1 - \frac{1}{1 + (Re/Re_0)^{\varepsilon}}, \quad Re = \frac{2\rho_0 U R}{\eta}, \tag{49}$$

and $Re_0 = 2000$ is the Reynolds number locating the transition region between the laminar and turbulent flow regime and the exponent ε is chosen in the present work. Substituting equation (48) into equation (40),

$$\begin{aligned} g(r) = {} & \frac{\eta U^2(\tau-1)}{\kappa_{th} R^4}\left((\beta\overline{T}_0 + 1)(1-\tau)r^4\right. \\ & \left. + 2\beta\overline{T}_0 R^2(\tau-2)r^2\right) \\ & - \frac{\eta U^2(\tau-1)}{\kappa_{th}}\left(1 - \tau + \beta\overline{T}_0(\tau-3)\right). \end{aligned} \tag{50}$$

In this section, the average flow profile is $U = 10\,\text{m/s}$. While Figure 2 shows the phase velocity of the first four modes propagation in incompressible viscous liquid fluid with shear flow $U = 10\,\text{m/s}$ for different rigid pipeline radii $R = 4\,\text{mm}$ and $R = 10\,\text{mm}$, Figure 3 presents the corresponding attenuation factor of the first and fourth modes. Clearly, phase velocity of higher modes in smaller pipeline radius is larger than that in larger smaller pipeline

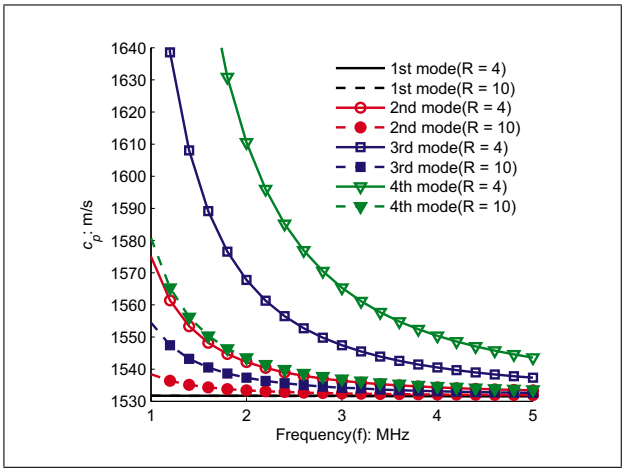


Figure 2. Dispersion curve of phase velocity for the first modes propagating in incompressible viscous liquid fluid with shear flow $U = 10\,\text{m/s}$ confined by rigid wall of $R = 4\,\text{mm}$ and $R = 10\,\text{mm}$.

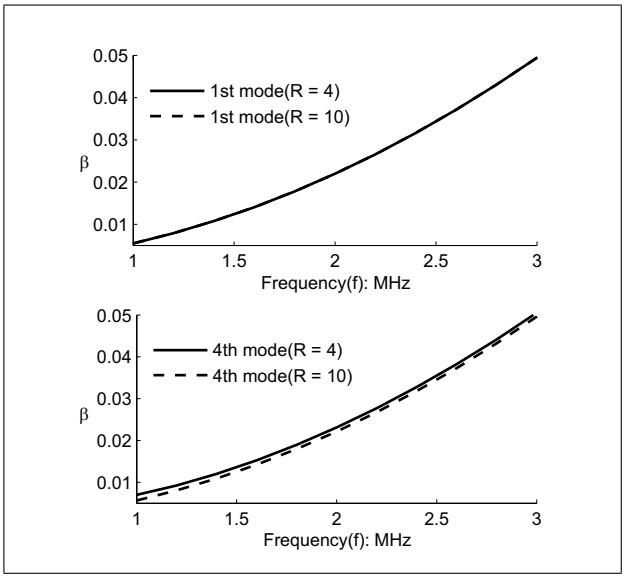


Figure 3. Attenuation factor of the first and fourth modes propagating in incompressible viscous fluid with shear flow $U = 10\,\text{m/s}$ confined by rigid wall of $R = 4\,\text{mm}$ and $R = 10\,\text{mm}$.

radius while phase velocity of the fundamental mode is independent on the pipeline radius as shown in Figure 2. Similarly, while attenuation factor for fundamental mode remains the same as acoustic frequency increases, attenuation factor of the higher mode turns out to be larger in pipeline with smaller radius. While phase velocity of each mode converges nonlinearly to a specific value of $c(\overline{T}_0) + U = 1531.5\,\text{m/s}$ in downstream propagation as acoustic frequency rises, attenuation factor increases nonlinearly.

As supplements, Figure 4 displays the phase velocity of the first four modes in downstream $U = 10\,\text{m/s}$ and upstream $U = -10\,\text{m/s}$ direction confined by rigid pipeline of $R = 4\,\text{mm}$, meanwhile Figure 5 illustrates the corresponding attenuation factor of the first and fourth modes

Document downloaded by @DAEL, 2026-11-08 02:50:09 - personal use only

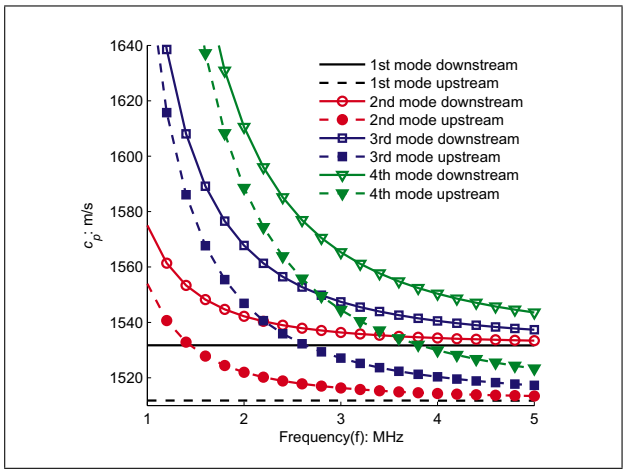


Figure 4. Dispersion curve of phase velocity for the first four modes propagating in downstream $U = 10$ m/s and upstream $U = -10$ m/s direction confined by rigid wall $R = 4$ mm.

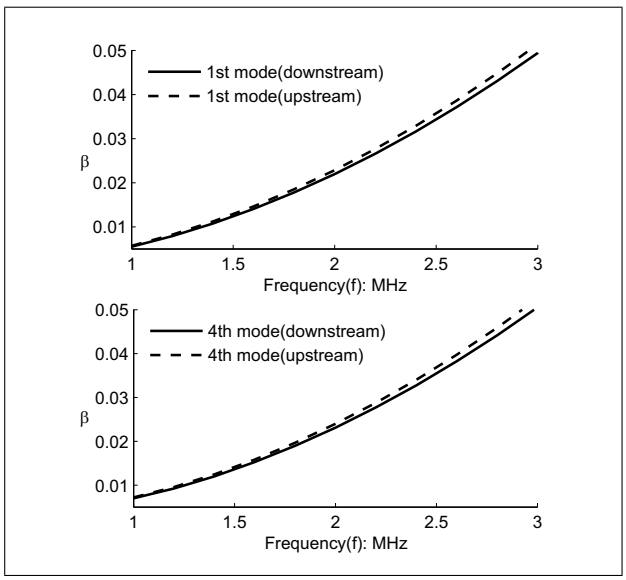


Figure 5. Attenuation factor of the first and fourth modes propagating in downstream direction $U = 10$ m/s and upstream direction $U = -10$ m/s confined by rigid pipeline of $R = 4$ mm.

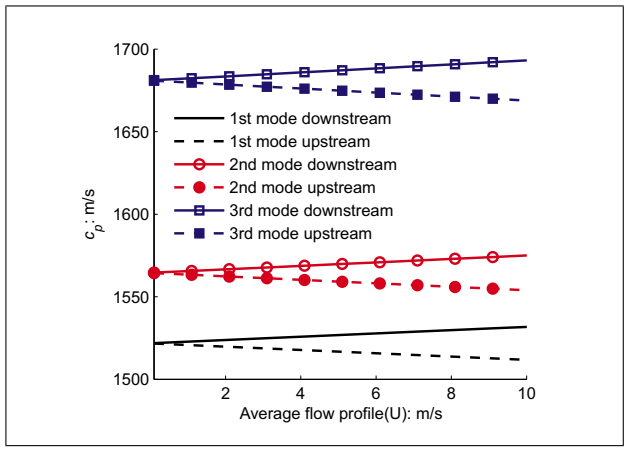


Figure 6. Phase velocity of the first three modes with acoustic frequency $f = 1$ MHz propagating in incompressible viscous fluid confined by rigid wall ($R = 4$ mm) in downstream and upstream direction as functions of average flow profile U.

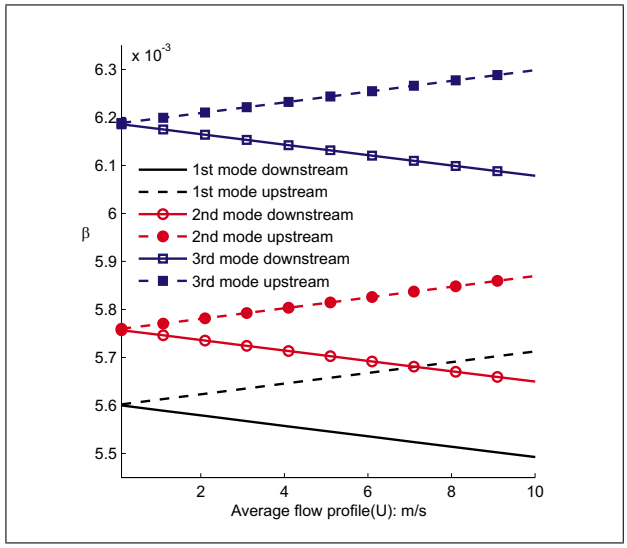


Figure 7. Attenuation factor of the first three modes with acoustic frequency $f = 1$ MHz propagating in incompressible viscous fluid confined by rigid wall ($R = 4$ mm) in downstream and upstream direction as functions of average flow profile U.

in downstream and upstream direction. In the downstream propagation, the convergent value of phase velocity is $c(\overline{T}_0) + U = 1531.5$ m/s while it becomes $c(\overline{T}_0) - U = 1511.5$ m/s in upstream propagation. From Figure 4, phase velocity of each mode is larger in downstream propagation than upstream propagation; on the other hand, attenuation factor of each mode shows smaller in downstream propagation than upstream propagation. Another point is that higher mode confronts severer attenuation which can also been seen in Figure 7.

In the end, Figures 6 and 7 demonstrate the phase velocity and attenuation factor of the first three modes propagation in downstream and upstream direction as functions of average flow profile where the acoustic frequency is $f = 1$ MHz and pipeline radius is $R = 4$ mm. In downstream propagation, phase velocity of each mode increases as average flow profile climbs up; however, attenuation factor of each mode declines. On the other hand, while phase velocity of each mode decreases with average flow profile, there are explicit increases in attenuation factor of each mode.

3.2. Measurement performance

In this section, measurement performance of ultrasonic flow meter in laminar and turbulent flow based on wave propagation is numerically analysed.

3.2.1. Laminar flow

Based on [21, 28, 29], the laminar flow profile can be described by Poisson'sequations, which can besolved analytically for circular pipelines, yielding

$$v_0(r) = 2U\left(1 - \frac{r^2}{R^2}\right). \tag{51}$$

Document downloaded by @DAEL, 2026-11-08 02:50:09 - personal use only

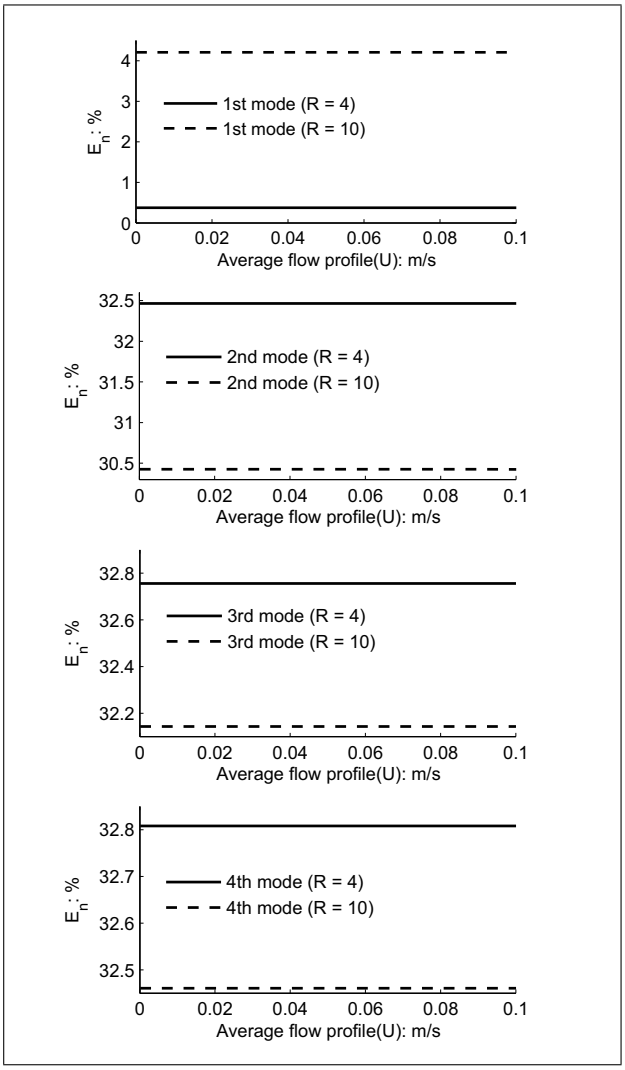


Figure 8. Measurement performance E_n of the first four modes for different pipeline radii $R = 4\,\text{mm}$ and $R = 10\,\text{mm}$ where the wall temperature is maintained at a constant value at $\overline{T}_0 = 293\,\text{K}$ while acoustic frequency is $f = 1\,\text{MHz}$ for laminar flow profile.

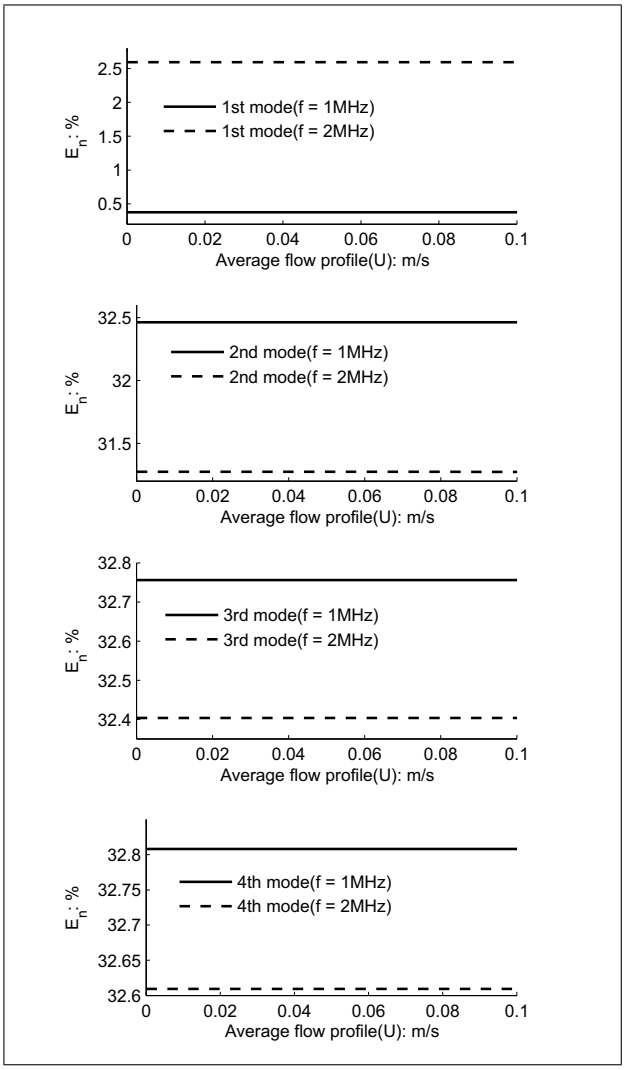


Figure 9. Measurement performance E_n of the first four modes for acoustic frequency $f = 1\,\text{MHz}$ and $f = 2\,\text{MHz}$ confined by rigid pipeline of $R = 4\,\text{mm}$ where the constant temperature at the wall is $\overline{T}_0 = 293\,\text{K}$ for laminar flow profile.

Substituting equation (51) into equation (40) gives the temperature distribution along the radius coordinate

$$g(r) = \frac{\eta U^2}{\kappa_{th} R^4}\left(4\beta\overline{T}_0 R^2 r^2 - (1 + 2\beta\overline{T}_0) r^4\right) - \frac{\eta U^2}{\kappa_{th}}\left(3\beta\overline{T}_0 - 1\right). \quad (52)$$

While Figure 8 demonstrates the deviation of measurement E_n of first four wave modes for different pipeline radii $R = 0.004\,\text{m}$ and $R = 0.01\,\text{m}$ where the acoustic frequency is $f = 1\,\text{MHz}$, Figure 9 denotes the corresponding deviation of measurement for different acoustic frequencies $f = 1\,\text{MHz}$ and $f = 2\,\text{MHz}$. Clearly, the measurement performance of fundamental mode is the best among the four wave modes, which is consistent with the work of Willatzen [83, 85, 86] in inviscid fluid with non-uniform shear flow. However, the difference is that while the deviation of measurement for the fundamental mode vanishes in inviscid fluid, the value in compressible thermal-viscous fluid does not vanish and varies with pipeline radius and acoustic frequency as shown in Figures 8 and 9. For specific radius and frequency, measurement error of higher wave mode is larger than lower wave mode. In different pipeline radii $R = 0.004\,\text{m}$ and $R = 0.01\,\text{m}$ where acoustic frequency is $f = 1\,\text{MHz}$, while measurement performance of fundamental mode is better in smaller radius, measurement error of larger radius is smaller for each high wave modes as shown in Figure 8. In specific radii $R = 0.004\,\text{m}$ of different acoustic frequency $f = 1\,\text{MHz}$ and $f = 2\,\text{MHz}$, fundamental wave mode with higher frequency performs worse than lower frequency, however, higher wave mode with higher frequency has better measurement quality than lower frequency as shown in Figure 9.

3.2.2. Turbulent flow

In this section, measurement performance of ultrasonic flow meter in turbulent flow isanalyzed where the turbu-

Document downloaded by @DAEL, 2026-11-08 02:50:09 - personal use only

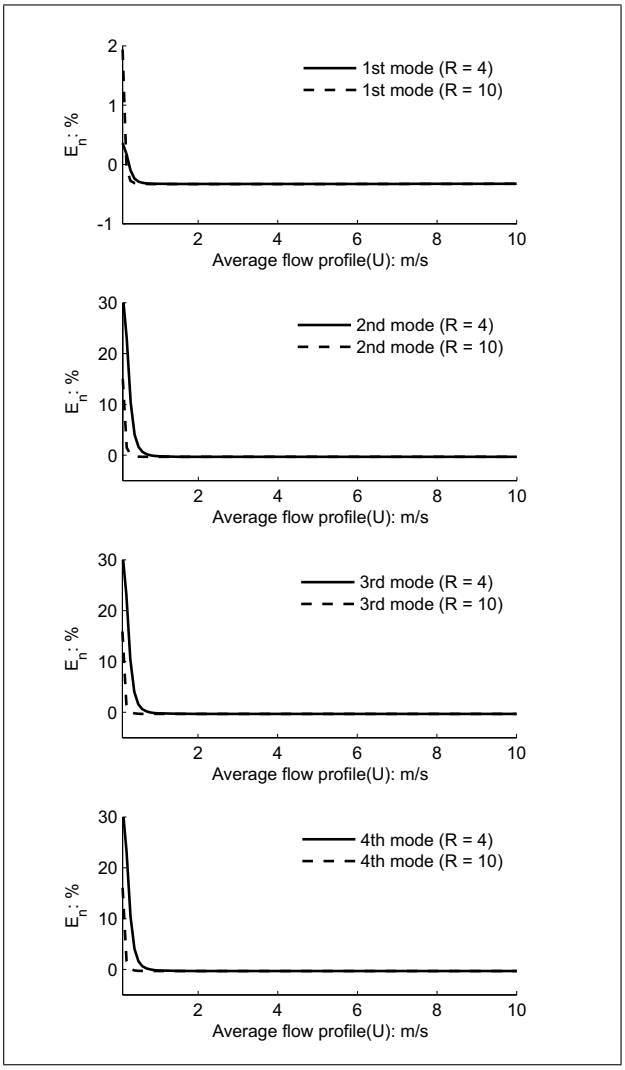


Figure 10. Measurement performance E_n of the first four modes for different pipeline radii $R = 4$ mm and $R = 10$ mm where the wall temperature is maintained at a constant value at $\overline{T}_0 = 293$ K while acoustic frequency is $f = 1$ MHz for turbulent flow profile.

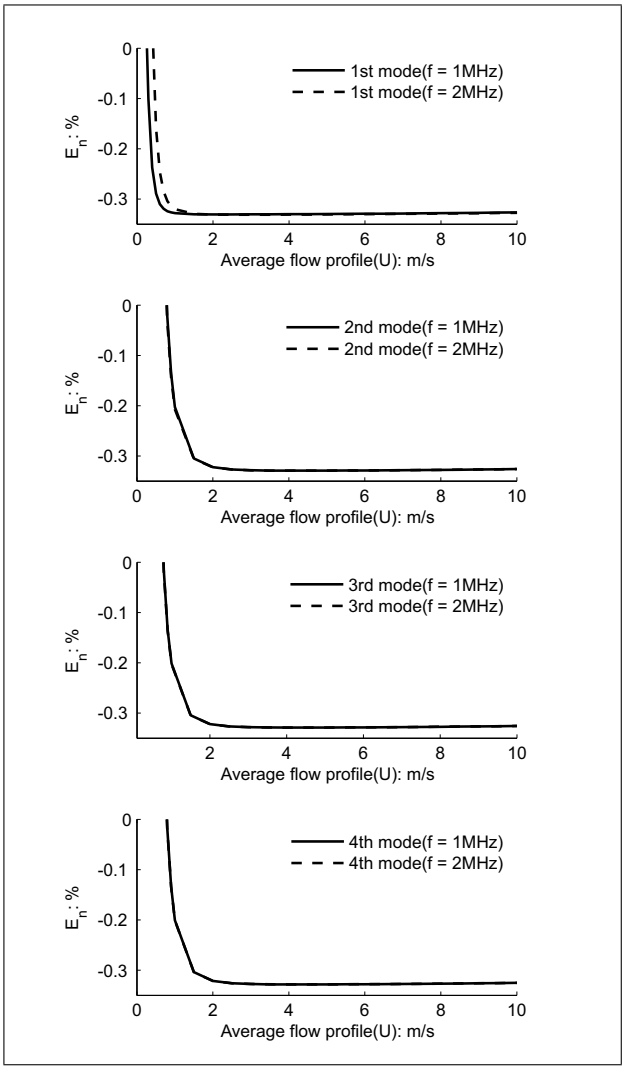


Figure 11. Measurement performance of the first four modes for acoustic frequency $f = 1$ MHz and $f = 2$ MHz confined by rigid pipeline of $R = 4$ mm where the constant temperature at the wall is $\overline{T}_0 = 293$ K for turbulent flow profile.

lent flow profile is shown in equation (48). To keep consistent with the analysis in laminar flow, Figure 10 details the measurement performance of the first four modes in different pipeline radii $R = 0.004$ m and $R = 0.01$ m for acoustic frequency $f = 1$ MHz, meanwhile Figure 11 draws the corresponding measurement performance of the first four modes in specific pipeline radii $R = 0.004$ m for acoustic frequency $f = 1$ MHz and $f = 2$ MHz.

Obviously, as average flow profile increases, measurement error converges to a specific value which is consistent with work of Willatzen [83, 85, 86] in inviscid fluid with non-uniform shear flow. However, in inviscid fluid, the convergent point is zero while the value in viscous fluid does not vanish for each mode as shown in Figure 11. In the turbulent flow profile in equation (48), measurement performance is independent on the pipeline radius and acoustic frequency as shown in Figures 10 and 11 which is similar in inviscid fluid. Moreover, measurement performance in larger radius or higher frequency converges more quickly. As shown in equation (48), in the case of low average flow profile, as the Reynolds number in equation (49) is lower, the laminar flow profile takes dominant in equation (48) and then measurement error is larger as shown in Figures 10 and 11. In higher average flow profile with larger Reynolds number, turbulent flow profile performs like uniform flow profile which corresponding to a constant measurement error for each wave.

4. Conclusion

Viscothermal longitudinal wave propagation in incompressible liquid fluid with non-uniform shear flow confined by rigid wall is mathematically deduced from conservations of continuity, momentum, and energy, which turns out to be a set of coupled fourth-order nonlinear differential equations. Based on the Bessel-Fourier theory, a general solution in the form of Bessel-Fourier sequences, which are orthogonal and complete in Lebesgue Space, is

Document downloaded by @DAEL, 2026-11-08 02:50:09 - personal use only

proposed to transform the fourth-order nonlinear differential equations to homogeneous linear algebraic equations. Moreover, the wave number, which represents the phase velocity and attenuation, can be solved using the existence condition of non-trivial solution of the proposed homogeneous linear algebraic equations, leading to the vanishment of the corresponding determinant which can be calculated using various numerical methods. In this paper, a parabolic Newton iteration method is introduced to solve the problem. In the end, phase velocity and attenuation is numerically studied in the presence of non-uniform shear flow, and meanwhile ultrasonic flow meter based on wave propagation is investigated in both laminar and turbulent flow.

Appendix

A1. Orthogonality of Bessel-Fourier theory

From the Bessel function theory [58], assume $J_\nu(\lambda_n r)$ and $J_\nu(\lambda_m r)$ are two solutions of the second-order differential equation

$$\begin{aligned} r^2\frac{\mathrm{d}^2 J_\nu(\lambda_n r)}{\mathrm{d}r^2} + r\frac{\mathrm{d}^2 J_\nu(\lambda_n r)}{\mathrm{d}r^2} \\ +\left(\lambda_n^2 r^2 - \nu^2\right) J_\nu(\lambda_n r) = 0, \\ r^2\frac{\mathrm{d}^2 J_\nu(\lambda_m r)}{\mathrm{d}r^2} + r\frac{\mathrm{d}^2 J_\nu(\lambda_m r)}{\mathrm{d}r^2} \\ +\left(\lambda_n^2 r^2 - \nu^2\right) J_\nu(\lambda_m r) = 0, \end{aligned} \tag{A1}$$

with $r \in [0, R]$ and $\nu \geq 0$. Dividing r^2 from equation (A.1) obtains

$$\begin{aligned} \frac{1}{r}\frac{\mathrm{d}}{\mathrm{d}r}\left(r\frac{\mathrm{d}J_\nu(\lambda_n r)}{\mathrm{d}r}\right) + \left(\lambda_n^2 - \nu^2/r^2\right) J_\nu(\lambda_n r) = 0, \\ \frac{1}{r}\frac{\mathrm{d}}{\mathrm{d}r}\left(r\frac{\mathrm{d}J_\nu(\lambda_m r)}{\mathrm{d}r}\right) + \left(\lambda_m^2 - \nu^2/r^2\right) J_\nu(\lambda_m r) = 0. \end{aligned} \tag{A2}$$

Multiplying $rJ_\nu(\lambda_m r)$ to the first and $rJ_\nu(\lambda_n r)$ to the second equation in equation (A.2) yields

$$\begin{aligned} J_\nu(\lambda_m r)\frac{\mathrm{d}}{\mathrm{d}r}\left(r\frac{\mathrm{d}J_\nu(\lambda_n r)}{\mathrm{d}r}\right) \\ +\left(\lambda_n^2 - \nu^2/r^2\right) rJ_\nu(\lambda_m r) J_\nu(\lambda_n r) = 0, \\ J_\nu(\lambda_n r)\frac{\mathrm{d}}{\mathrm{d}r}\left(r\frac{\mathrm{d}J_\nu(\lambda_m r)}{\mathrm{d}r}\right) \\ +\left(\lambda_m^2 - \nu^2/r^2\right) rJ_\nu(\lambda_m r) J_\nu(\lambda_n r) = 0, \end{aligned} \tag{A3}$$

subtracting the second equation from the first gives

$$\begin{aligned} \left(\lambda_m^2 - \lambda_n^2\right) rJ_\nu(\lambda_m r) J_\nu(\lambda_n r) = \\ J_\nu(\lambda_m r)\frac{\mathrm{d}}{\mathrm{d}r}\left(r\frac{\mathrm{d}J_\nu(\lambda_n r)}{\mathrm{d}r}\right) \\ -J_\nu(\lambda_n r)\frac{\mathrm{d}}{\mathrm{d}r}\left(r\frac{\mathrm{d}J_\nu(\lambda_m r)}{\mathrm{d}r}\right), \end{aligned} \tag{A4}$$

integrating over $[0, R]$ yields

$$\begin{aligned} \left(\lambda_m^2 - \lambda_n^2\right)\int_0^R J_\nu(\lambda_m r) J_\nu(\lambda_n r)\, r\,\mathrm{d}r = \\ \int_0^R \left[J_\nu(\lambda_m r)\frac{\mathrm{d}}{\mathrm{d}r}\left(r\frac{\mathrm{d}J_\nu(\lambda_n r)}{\mathrm{d}r}\right)\right. \\ \left. -J_\nu(\lambda_n r)\frac{\mathrm{d}}{\mathrm{d}r}\left(r\frac{\mathrm{d}J_\nu(\lambda_m r)}{\mathrm{d}r}\right)\right] r\,\mathrm{d}r. \end{aligned} \tag{A5}$$

Integration by parts obtains

$$\begin{aligned} \left(\lambda_m^2 - \lambda_n^2\right)\int_0^R J_\nu(\lambda_m r) J_\nu(\lambda_n r)\, r\,\mathrm{d}r = \\ \left(rJ_\nu(\lambda_m r)\frac{\mathrm{d}J_\nu(\lambda_n r)}{\mathrm{d}r} - rJ_\nu(\lambda_n r)\frac{\mathrm{d}J_\nu(\lambda_m r)}{\mathrm{d}r}\right)\Bigg|_0^R. \end{aligned} \tag{A6}$$

Then there is

$$\begin{aligned} \left(\lambda_m^2 - \lambda_n^2\right)\int_0^R J_\nu(\lambda_m r) J_\nu(\lambda_n r)\, r\,\mathrm{d}r = \\ R\left(J_\nu(\lambda_m R)\frac{\mathrm{d}J_\nu(\lambda_n r)}{\mathrm{d}r} - J_\nu(\lambda_n r)\frac{\mathrm{d}J_\nu(\lambda_m r)}{\mathrm{d}r}\right). \end{aligned} \tag{A7}$$

For λ_n, $n = 1, 2, 3\ldots$ satisfying the constraints

$$\frac{\mathrm{d}J_\nu(\lambda_n r)}{\mathrm{d}r} = 0 \quad \text{or} \quad J_\nu(\lambda_n R) = 0, \tag{A8}$$

equation (A7) can be simplified to be

$$\left(\lambda_m^2 - \lambda_n^2\right)\int_0^R J_\nu(\lambda_m r) J_\nu(\lambda_n r)\, r\,\mathrm{d}r = 0, \tag{A9}$$

as a result, for Bessel functions $J_\nu(\lambda_n r)$ and $J_\nu(\lambda_m r)$ with $m \neq n$, $\lambda_n(\lambda_m)$ satisfying equation (A.8), the following condition holds

$$\int_0^R J_\nu(\lambda_m r) J_\nu(\lambda_n r)\, r\,\mathrm{d}r = 0, \tag{A10}$$

which shows the orthogonality of Bessel sequence over $[0, R]$ in Lebesgue Space $\mathcal{L}_r^2(0, R)$.

On the other hand, for $m = n$, $\int_0^R J_\nu^2(\lambda_n r)\, r\,\mathrm{d}r$ cannot be obtained from equation (A.9) because the term $(\lambda_m^2 - \lambda_n^2)$ in the left side vanishes. To find the integration of $\int_0^R J_\nu^2(\lambda_n r)\, r\,\mathrm{d}r$, firstly, multiplying $r^2\mathrm{d}J_\nu(\lambda_n r)/\mathrm{d}r$ to the first equation in equation (A.3) gives

$$\begin{aligned} r\frac{\mathrm{d}J_\nu(\lambda_n r)}{\mathrm{d}r}\frac{\mathrm{d}}{\mathrm{d}r}\left(r\frac{\mathrm{d}J_\nu(\lambda_n r)}{\mathrm{d}r}\right) \\ +\left(\lambda_n^2 r^2 - \nu^2\right) J_\nu(\lambda_n r)\frac{\mathrm{d}J_\nu(\lambda_n r)}{\mathrm{d}r} = 0. \end{aligned} \tag{A11}$$

Integrating over $[0, R]$ obtains

$$\begin{aligned} \frac{1}{2}\left(r\frac{\mathrm{d}J_\nu(\lambda_n r)}{\mathrm{d}r}\right)\Bigg|_0^R \\ +\int_0^R \left(\lambda_n^2 r^2 - \nu^2\right) J_\nu(\lambda_n r)\frac{\mathrm{d}J_\nu(\lambda_n r)}{\mathrm{d}r}\mathrm{d}r = 0. \end{aligned} \tag{A12}$$

Document downloaded by @DAEL, 2026-11-08 02:50:09 - personal use only

Integration by parts yields

$$\frac{1}{2}\left(r\frac{\mathrm{d}J_\nu(\lambda_n r)}{\mathrm{d}r}\right)\Big|_0^R + \frac{1}{2}\left(\lambda_n^2 r^2 - \nu^2\right)J_\nu(\lambda_n r)\Big|_0^R - \lambda_n^2\int_0^R J_\nu^2(\lambda_n r)\, r\,\mathrm{d}r = 0, \tag{A13}$$

thus we have

$$\int_0^R J_\nu^2(\lambda_n r)\, r\,\mathrm{d}r = \frac{1}{2\lambda_n^2}\left[\left(r\frac{\mathrm{d}J_\nu(\lambda_n r)}{\mathrm{d}r}\Big|_0^R\right)^2 + \left(\lambda_n^2 R^2 - \nu^2\right)J_\nu(\lambda_n R)\right], \tag{A14}$$

as

$$\frac{\mathrm{d}J_\nu(\lambda_n r)}{\mathrm{d}r} = \frac{\nu}{r}J_\nu(\lambda_n r) - \lambda_n J_{\nu+1}(\lambda_n r), \tag{A15}$$

then we have

$$\int_0^R J_\nu^2(\lambda_n r)\, r\,\mathrm{d}r = \frac{1}{2\lambda_n^2}\left[\left(\frac{\nu}{\lambda_n}J_\nu(\lambda_n R) - R\lambda_n J_{\nu+1}(\lambda_n R)\right)^2 + \left(\lambda_n^2 R^2 - \nu^2\right)J_\nu(\lambda_n R)\right]. \tag{A16}$$

Furthermore, the verification of completeness of Bessel-Fourier sequence $J_\nu(\lambda_n R)$, where λ_n satisfies equation (A8), can be seen in Al-Gwaiz [58].

A2. Parabolic Newton iteration method

In this appendix, parabolic Newton method is introduced to find a solution of a nonlinear algebraic equation

$$f(z) = 0, \tag{A17}$$

where $z \in \mathbf{C}$. Previous research can be seen in [88, 89, 90, 91].

For an initial point z_k, using Taylor's expansion leads to

$$f(z) = f(z_k) + f'(z_k)(z - z_k) + \frac{1}{2!}f^n(z_k)(z - z_k)^2 + \ldots \tag{A18}$$

omitting the order higher than three, there is

$$f(z) = f(z_k) + f'(z_k)(z - z_k) + \frac{1}{2!}f^n(z_k)(z - z_k)^2, \tag{A19}$$

if point z_{k+1} is the root of equation (A17), then there is $f(z_{k+1}) = 0$, substituting into equation (A19) yields

$$f(z_k) + f'(z_k)(z_{k+1} - z_k) + \frac{1}{2!}f^n(z_k)(z_{k+1} - z_k)^2 = 0. \tag{A20}$$

As a result, it can be deduced that

$$z_{k+1} = z_k - \frac{f'(z_k) - \sigma\sqrt{\left(f'(z_k)\right)^2 - 2f(z_k)f''(z_k)}}{f''(z_k)}, \tag{A21}$$

where $\sigma = \pm 1$. To get a faster convergent iteration, σ is selected to get a smaller value of $|f(z_{k+1})|$ at every iteration.

Acknowledgement

The work described in this paper is funded by the National Natural Science Foundation of China (No. 9126201 and 51205403). The authors gratefully acknowledge the funding.

References

[1] Lord Rayleigh: Theory of sound. Macmillan, London, 1896.

[2] C. Zwikker, C. Kosten: Sound absorbing materials. Elsevier, Amsterdam, 1949.

[3] P. N. Liang, H. A. Scarton: Attenuation of higher order circumferential thermoacoustic waves in viscous fluid lines. J. Sound Vib. **193** (1996) 1099–1113.

[4] W. M. Beltman: Viscothermal wave propagation including acousto-elastic interaction. Part 1: Theory. J. Sound Vib. **227** (1999) 555–586.

[5] W. M. Beltman: Viscothermal wave propagation including acousto-elastic interaction. Part ii: Application. J. Sound Vib. **227** (1999) 587–609.

[6] E. Rodarte, G. Singh, N. R. Miller, P. Hrnjak: Sound attenuation in tubes due to visco-thermal effects. J. Sound Vib. **231** (2000) 1221–1242.

[7] R. I. Sujith, G. A. Waldherr, B. T. Zinn: An exact solution for one-diemnsional acoustic fields in ducts with an axial temperature gradient. J. Sound Vib. **184** (1995) 389–402.

[8] J. Hoffelner, H. Landes, M. Kaltenbacher, R. Lerch: Finite element simulation of nonlinear wave propagation in thermoviscous fluids including dissipation. IEEE Trans. Ultrason., Ferroelect., Freq. Contr. **48** (2001) 779–786.

[9] G. C. Gaunaurd, G. C. Everstine: Viscosity effects on the propagation of acoustic transients. J. Vib. Acoust. **124** (2002) 19–25.

[10] K. S. Peat: A first approximation to the effects of mean flow on sound propagation through cylindrical capillary tubes. J. Sound Vib. **175** (1994) 475–489.

[11] K. S. Peat: Convected acoustic wave motion along a capillary duct with an axial temperature gradient. J. Sound Vib. **203** (1997) 855–866.

[12] K.-W. Jeong, J.-G. IH: A numerical study on the propagation of sound through capillary tubes with mean flow. J. Sound Vib. **198** (1996) 67–79.

[13] R. J. Astley, A. Cummings: Wave propagation in catalytic converters: formulation of the problem and finite element solution scheme. J. Sound Vib. **188** (1995) 635–657.

[14] J.-G. IH, C.-M. Park, H.-J. Kim: A model for sound propagation in capillary ducts with mean flow. J. Sound Vib. **190** (1996) 163–175.

[15] E. Dokumaci: Sound transmission in narrow pipes with superimposed uniform mean flow and acoustic modelling of autombile catalytic converters. J. Sound Vib. **182** (1995) 799–808.

[16] E. Dokumaci: An approximate dispersion equation for sound waves in a narrow pipe with ambient gradients. J. Sound Vib. **240** (2001) 637–646.

[17] E. Dokumaci: On transmission of sound in circular and rectangular narrow pipes with superimposed mean flow. J. Sound Vib. **210** (1998) 375–389.

[18] M. Willatzen: Phase shift and attenuation characteristics of acoustic waves in a flowing gas confined by cylindrical walls. J. Sound Vib. **261** (2003) 791–803.

Document downloaded by @DAEL, 2026-11-08 02:50:09 - personal use only

[19] E. Dokumaci: On attenuation of plane sound waves in turbulent mean flow. J. Sound Vib. **320** (2009) 1131–1136.

[20] M. Knutsson, M. Abom: Sound propagation in narrow tubes including effects of viscothermal and turbulent damping with application to chargeaircoolers. J. Sound Vib. **320** (2009) 289–321.

[21] M. Knutsson, M. Abom: The effect of turbulence damping on acoustic wave propagation in tubes. J. Sound Vib. **329** (2010) 4719–4739.

[22] M. S. Howe: The damping of sound by wall turbulent shear layers. J. Acoust. Soc. Am. **98** (1995) 1723–1730.

[23] W. Eversman, E. L. Cook, R. J. Beckemeyer: A method of weighted residuals for the investigation of sound transmission in non-uniform ducts without flow. J. Sound Vib. **38** (1975) 105–123.

[24] P. T. Vo, W. Eversman: A method of weighted residuals with trigonometric basis functions for sound transmission in circular ducts. J. Sound Vib. **56** (1978) 243–250.

[25] R. J. Astley, W. Eversman: A finite element method for transmission in non-uniform ducts without flow: comparison with the method of weighted residuals. J. Sound Vib. **57** (1978) 367–388.

[26] W. Eversman, R. J. Astley: Acoustic transmission in nonuniform ducts with mean flow. Part I: The method of weighted residuals. J. Sound Vib. **74** (1981) 89–101.

[27] K. S. Peat, R. Kirby: Acoustic wave motion along a narrow cylindrical duct in the presence of an axial mean flow and temperature gradient. J. Acoust. Soc. Am. **107** (2000) 1859–1867.

[28] L. D. Landau, E. M. Lifshitz: Fluid mechanics. Pergamon Press, Oxford, England, 1987.

[29] A. L. Fetter, J. D. Walecka: Theoretical mechanics of particles and continua. McGraw-Hill, New York, 2003.

[30] F. M. White: Viscous fluid flow. McGraw-Hill, New York, 1991.

[31] L. Elvira-Segura: Acoustic wave dispersion in a cylindrical elastic tube filled with a viscous liquid. Ultrasonics **37** (2000) 537–547.

[32] K. Baik, J. Jiang, T. G. Leighton: Acoustic attenuation, phase and group velocities in liquid-filled pipes: theory, experiment, and examples of water and mercury. J. Acoust. Soc. Am. **128** (2010) 2610–2624.

[33] S. V. Sorokin, A. V. Chubinskij: On the role of fluid viscosity in wave propagation in elastic plates under heavy fluid loading. J. Sound Vib. **311** (2008) 1020–1038.

[34] S. G. Kadyrov, J. Wauer, S. V. Sorokin: A potential technique in the theory of interaction between a structure and a viscous, compressible fluid. Arch. Appl. Mech. **71** (2001) 405–417.

[35] Y. Chen, Y. Huang, X. Chen: Acoustic propagation in viscous fluid with uniform flow and a novel design methodology for ultrasonic flow meter. Ultrasonics **53** (2013) 595–606.

[36] M. Willatzen: Temperaure gradients and flow-meter performance. Ultrasonics **39** (2001) 383–389.

[37] M. Willatzen: Ultrasonic flowmeters: temperature gradients and transducer geometry effects. Ultrasonics **41** (2003) 105–114.

[38] P. Holstein, A. Raabe, R. Muller, M. Barth, D. Mackenzie, E. Starke: Acoustic tomography on the basis of travel-time measurement. Meas. Sci. Technol. **15** (2004) 1420–1428.

[39] G. A. Jackson, J. R. Gibson, R. Holmes: A three-path ultrasonic flow meter with fluid velocity profile identification. Meas. Sci. Technol. **2** (1991) 635–642.

[40] G. A. Jackson, J. R. Gibson, R. Holmes: A three-path ultrasonic flowmeter for small-diameter pipelines. Meas. Sci. Technol. **22** (1989) 645–650.

[41] P. I. Moore, G. J. Brown, B. P. Stimpson: Ultrasonic transit-time flowmeters modelled with theoretical velocity profiles: methodology. Meas. Sci. Technol. **11** (2000) 1802–1811.

[42] F. Schneider, F. Peters, W. Merzkirch: Quantitative analysis of the cross-correlation ultrasonic flow meter by means of system theory. Meas. Sci. Technol. **14** (2003) 573–582.

[43] Y. Chen, J. Fu, Y. Huang, Y. Zhao, L. Cao, X. Chen, J. Fan: Ultrasonic flow meter for propellant on-orbit gauging based on folded multi-tone phase measurement: model analysis. – In: American Control Conference. T. Samad (ed.). Montréal, Québec, Canada, 2012, 4010–4015.

[44] H. Sato, H. Ogiso: Theoretical and simulated analysis of guided waves propagating in fluid-filled pipes. Jpn. J. Appl. Phys. **49** (2010) 07HC08.

[45] C. Wang, L. Huang: Time-domain simulation of acoustic wave propagation and interaction with flexible structures using chebyshev collocation method. J. Sound Vib. **331** (2012) 4343–4358.

[46] D. C. Gazis: Three-dimensional investigation of the propagation of waves in hollow circular cylinders. I. Analytical foundation. J. Acoust. Soc. Am. **31** (1959) 568–573.

[47] P.-C. Eccardt, H. Landes, R. Lerch: Finite element simulation of acoustic wave propagation within flowing media. IEEE International Ultrasonics Symposium, 1996, 991–994.

[48] A. Modinos, N. Stefanou, I. E. Psarobas, V. Yannopapas: On wave propagation in inhomogenous systems. Phys. B **296** (2001) 167–173.

[49] E. Ovalle, R. Araya, F. Concha: The role of wave propagation in hydrocyclone operations I: An axisymmetric streamfunction formulation. Chem. Engng. J. **111** (2005) 205–211.

[50] H. Sato, M. Lebedev, J. Akedo: Theoretical and experimental investigation of propagation of guide waves in cylindrical pipe filled with fluid. Jap. J. Appl. Phys. **45** (2006) 4573–4576.

[51] H. Sato, M. Lebedev, J. Akedo: Theoretical investigation of guide wave flowmeter. Jap. J. Appl. Phys. **46** (2007) 4521–4528.

[52] P. B. Nagy, A. H. Nayfeh: Viscosity-induced attenuation of longitudinal guided waves in fluid-loaded rods. J. Acoust. Soc Am. **100** (1996) 1501–1508.

[53] S. X. Liu, Z. J. Wu, L. G. Tang, X. M. Xu: Data transfer using the low frequency longitudinal guided wave in a liquid-filled pipe. Appl. Acoust. **73** (2012) 158–163.

[54] B.-G. Loh, D.-R. Lee: Heat transfer characteristics of acoustic streaming by longitudinal ultrasonic vibration. J. Acoust. Soc Am. **18** (2004) 94–99.

[55] H. Kwun, K. A. Bartels, C. Dynes: Dispersion of longitudinal waves propagating in liquid-filled cylindrical shells. J. Acoust. Soc. Am. **105** (1999) 2601–2611.

[56] S. Hassani: Mathematical methods: for students of physics and related fields. Springer-Verlag, New York, 2008.

[57] G. Arfken: Mathematical methods for physicists. Academic Press, San Diego, California, 1985.

[58] M. A. Al-Gwaiz: Sturm-Liouville theory and its applications. Springer-Verlag, London, 2008.

Document downloaded by @DAEL, 2026-11-08 02:50:09 - personal use only

[59] J. R. Higgins: Completeness and basis properties of sets of special functions. Cambridge University Press, London, 2004.

[60] H. J. Weber, G. B. Afrken: Essential mathematical methods for physicists. Academic Press, United States of America, 2003.

[61] A. Baricz: Generalized Bessel functions of the first kind. Springer-Verlag, London, New York, Berlin, Heidelberg, 2010.

[62] F. W. J. Olver, D. W. Lozier, R. F. Boizvert, C. W. Clark: NIST Handbook of mathematical functions. Cambridge University Press, New York, 2010.

[63] A. P. Prudnikov, Y. A. Brychkov, O. I. Marichev: Integrals and series II. Special functions. Gordon and Breach Science Publishers, New York, 1992.

[64] G. N. Watson: A treatise on the theory of Bessel functions. Cambridge University Press, London, 1966.

[65] I. S. Gradshteyn, I. M. Ryzhik: Table of integrals, series, and products. Academic Press, Burlington, USA, 2007.

[66] O. J. Farrell, B. Ross: Solved problems in analysis as applied to Gamma, Beta, Legendre and Bessel functions. Dover, New York, 1971.

[67] B. G. Korenev: Bessel functions and their applications. Taylor and Franics, London and New Yord, 2002.

[68] S. S. Phull: A definite integral for Bessel's function. Amer. Math. Monthly **46** (1969) 549–551.

[69] A. Laforgia: Inqualities for Bessel functions. J. Comput. Appl. Math. **15** (1986) 75–81.

[70] A. Elbert: An approximation for the zeros of Bessel functions. Numer. Math. **59** (1991) 647–657.

[71] V. Barsan, S. Cojocaru: Physical applications of a simple approximation of Bessel functions of integer order. Eur. J. Phys. **28** (2007) 983–989.

[72] A. Laforgia, P. Natalini: Zeros of Bessel functions: monotonicity, concavity, inequalities. Le Matematiche **LXII** (2007) 255–270.

[73] T. S. Shores: Applied linear algebra and matrix analysis. Springer, New York, 2007.

[74] D. S. Watkins: Fundamentals of matrix computations. John Wiley, New York, 2002.

[75] C. D. Meyer: Matrix analysis and applied linear algebra. SIAM, New York, 2001.

[76] R. A. Horn, C. R. Johnson: Matrix analysis. Cambridge University Press, Cambridge, 1985.

[77] D. Blokhintzev: The propagation of sound in an inhomogeneous and moving medium I. J. Acoust. Soc. Am. **18** (1946) 322–328.

[78] H. Tijdeman: On the propagation of sound waves in cylindrical tubes. J. Sound Vib. **39** (1975) 1–33.

[79] K. A. Kousen: Eigenmodes of ducted flows with radially-dependent axial and swirl velocity components. NASA Report, CR-1999-208881, 1999.

[80] J. D. Achenbach: Wave propagation in elastic solids. North-Holland Publishing Company, London, 1973.

[81] D. R. Lide: Handbook of chemistry and physics. CRC Press, USA, 2002.

[82] L. Wang, K. L. McCarthy, M. J. McCarthy: Effect of temperature gradient on ultrasonic Doppler velocimetry measurement during pipe flow. Food Res. Int. **37** (2004) 633–642.

[83] M. Willatzen: Sound propagation in a moving fluid confined by cylindrical walls – a comparison between an exact analysis and the local-plane wave approximation. J. Sound Vib. **247** (2001) 719–729.

[84] M. Willatzen: Comments on "Ultrasonic flow metering based on transit time differentials which are insensitive to flow profile". J. Acoust. Soc. Am. **107** (2000) 1762–1765.

[85] M. Willatzen: Perturbation theory applied to sound propagation in flowing media confined by a cylindrical waveguide. J. Acoust. Soc. Am. **109** (2001) 102–107.

[86] M. Willatzen: Flow acoustics modelling and implications for ultrasonic flow measurement based on the transit-time method. Ultrasonics **41** (2004) 805–810.

[87] M. Willatzen: Liquid flows and vibration characteristics of straight-tube cylindrical shells. J. Sound Vib. **260** (2003) 417–429.

[88] L. Yau, A. Ben-Israel: The Newton and Halley methods for complex roots. Am. Math. Mon. **105** (1998) 806–818.

[89] C. A. Neff, J. H. Reif: An efficient algorithm for the complex roots problem. J. Compl. **12** (1996) 81–115.

[90] H. Hubbard, D. Schleicher, S. Sutherland: How to find all roots of complex polynomials by Newton's method. Invent. Math. **146** (2001) 1–33.

[91] D. E. Muller: A method for solving algebraic equations using an automatic computer. Math. Tables Aids Comput. **10** (1956) 208–215.

Document downloaded by @DAEL, 2026-11-08 02:50:09 - personal use only